

Gas-Phase Acidities Derived from Threshold Energies for Activated Reactions

Susan T. Graul[†] and Robert R. Squires*

Contribution from the Department of Chemistry, Purdue University, West Lafayette, Indiana 47907. Received August 18, 1989

Abstract: Appearance energies have been measured for the ionic products from activated unimolecular dissociations of organic carboxylate ions, alkoxide ions, and ketone enolates as well as for products from endothermic bimolecular proton-transfer and nucleophilic displacement reactions. A correlation between the experimental energies of the reaction onsets and the reaction endothermicity permits the derivation of gas-phase acidities for the conjugate acids of the product carbanions by means of simple thermochemical cycles. The acidities so derived generally show good agreement with literature values or with predictions based on analogous systems, although certain of the reactions display threshold energies higher than what would be predicted from the reaction enthalpy, due to activation barriers or kinetic shifts, whereas others have threshold energies lower than expected. These latter systems have the common characteristic of acidic hydrogens in the side chain of the reactant ions, leading to the possibility of isomerization. General features of the collisional activation experiments and the data analysis are described. Gas-phase acidities are derived for methane, fluoromethane, ethylene, cyclopropane, and neopentane, as well as several other species.

The acidity of a compound is a fundamental property from which many predictions can be made about the reactivity of that compound and of its conjugate base. Consequently, numerous studies have been devoted to determining acidities both in solution¹⁻⁵ and in the gas phase.^{4,6-10} Well-established methods for the determination of gas-phase acidities include measurements of bimolecular proton-exchange equilibria or of the kinetics of forward and reverse proton-transfer reactions, as well as acidity bracketing.^{6,7} Such techniques obviously require that proton abstraction occurs to a measurable extent on the time scale of the experiment and, although widely applicable, suffer from the limitation that they probe only the most acidic hydrogen or hydrogens in a compound and generally are not useful for species that are less acidic than ammonia [$\Delta H_{\text{acid}}(\text{NH}_3) = 403.6$ kcal/mol].⁷ Gas-phase acidities can sometimes be measured by alternative methods that do not require the occurrence of a bimolecular proton transfer and thus circumvent the need for basic and/or selective reagent ions. For example, the acidity of methane [$\Delta H_{\text{acid}}(\text{CH}_4) = 416.6$ kcal/mol]⁷ has been derived via a thermochemical cycle (eq 1, R = CH₃) from the experimental bond

$$\Delta H_{\text{acid}}(\text{RH}) = \text{IP}(\text{H}) + D[\text{R}-\text{H}] - \text{EA}(\text{R}) \quad (1)$$

dissociation energy of methane ($D[\text{CH}_3-\text{H}] = 104.8$ kcal/mol)¹¹ and the measured electron affinity of the methyl radical ($\text{EA} = 1.8$ kcal/mol).¹² DePuy and co-workers recently developed a kinetic method for the determination of hydrocarbon acidities that does not require the production of a free carbanion and that moreover can be used to estimate the acidity at virtually any site in an alkane.¹³ In this method, the branching ratio for displacement of RH or CH₄ from the reaction of OH⁻ with alkyltrimethylsilanes RSiMe₃ is correlated with the relative gas-phase acidities of the alkane RH and methane. They have reported acidities determined by this technique for a number of organic compounds, including acyclic, cyclic, and unsaturated hydrocarbons.¹³

In the preceding paper in this issue, we presented results from our general survey of the collisionally activated unimolecular dissociations of organic carboxylate ions RCO₂⁻.¹⁴ These investigations grew out of a study of the structures and reactivity of the C₃H₅⁻ fragment ions produced from collision-induced decarboxylation of a series of isomeric C₃H₅CO₂⁻ ions.¹⁵ We have adapted the method for use in a flowing afterglow-triple quadrupole instrument and have employed decarboxylation as a preparative method in studies of the reactivity of the methyl anion CH₃⁻ and of the stability of gas-phase alkyl anions with respect

to electron detachment.^{14,16} The reverse reaction, addition of an anion to CO₂, is believed to proceed essentially without barrier for many ions.^{17,18} If this is true, then the height of any barrier along the dissociation pathway yielding R⁻ and CO₂ cannot exceed the energy of the separated R⁻ and CO₂ species. Under such circumstances, it seems plausible that a correlation will exist between the enthalpy change for decarboxylation and the experimental activation energy for dissociation of an ensemble of RCO₂⁻ ions that, prior to activation, is of a well-characterized internal energy. Therefore, we set out to examine the energetics for decarboxylation of thermal energy RCO₂⁻ ions selected from the flow tube (300 K) to determine whether the experimental appearance energy for the fragment R⁻ correlated with the enthalpy change for decarboxylation. We reported our preliminary results in an earlier communication¹⁹ and herein augment and

(1) Cram, D. J. *Fundamentals of Carbanion Chemistry*; Academic Press: New York, 1965.

(2) Bordwell, F. G. *Pure Appl. Chem.* **1977**, *49*, 963.

(3) Streitwieser, A., Jr.; Juaristi, E.; Nebenzahl, L. L. In *Comprehensive Carbanion Chemistry, Part A*; Bunzel, E.; Durst, T., Eds.; Elsevier: Amsterdam, 1980; Chapter 7.

(4) Taft, R. W. *Prog. Phys. Org. Chem.* **1983**, *14*, 247.

(5) Jorgensen, W. L.; Briggs, J. M. *J. Am. Chem. Soc.* **1989**, *111*, 4190.

(6) Bartmess, J. E.; McIver, R. T., Jr. In *Gas-Phase Ion Chemistry*; Bowers, M. T., Ed.; Academic Press: New York, 1979; Vol. 2, Chapter 11.

(7) Lias, S. G.; Bartmess, J. E.; Liebman, J. F.; Holmes, J. L.; Levin, R. D.; Mallard, W. G. *J. Phys. Chem. Ref. Data* **1988**, *17*, Suppl. 1.

(8) Kollmar, H. *J. Am. Chem. Soc.* **1978**, *100*, 2665.

(9) Gordon, M. S.; Davis, L. P.; Burggraf, L. W.; Damrauer, R. *J. Am. Chem. Soc.* **1986**, *108*, 7889.

(10) Siggel, M. R. F.; Thomas, T. D.; Saethre, L. J. *J. Am. Chem. Soc.* **1988**, *110*, 91.

(11) Russell, J. J.; Seetula, J. A.; Gutman, D. *J. Am. Chem. Soc.* **1988**, *110*, 3092.

(12) Ellison, G. B.; Engelking, P. C.; Lineberger, W. C. *J. Am. Chem. Soc.* **1978**, *100*, 2556.

(13) (a) DePuy, C. H.; Bierbaum, V. M.; Damrauer, R. *J. Am. Chem. Soc.* **1984**, *106*, 4051. (b) DePuy, C. H.; Gronert, S.; Barlow, S. E.; Bierbaum, V. M.; Damrauer, R. *J. Am. Chem. Soc.* **1989**, *111*, 1968.

(14) Graul, S. T.; Squires, R. R. *J. Am. Chem. Soc.*, preceding article in this issue.

(15) Froelicher, S. W.; Freiser, B. S.; Squires, R. R. *J. Am. Chem. Soc.* **1986**, *108*, 2853.

(16) Graul, S. T.; Squires, R. R. *J. Am. Chem. Soc.* **1989**, *111*, 892.

(17) (a) Bierbaum, V. M.; DePuy, C. H.; Shapiro, R. H. *J. Am. Chem. Soc.* **1977**, *99*, 5800. (b) Bierbaum, V. M.; Grabowski, J. J.; DePuy, C. H. *J. Chem. Phys.* **1984**, *88*, 1389. (c) DePuy, C. H. *Org. Mass Spectrom.* **1985**, *20*, 556.

(18) Liang, J.-Y.; Lipscomb, W. N. *J. Am. Chem. Soc.* **1986**, *108*, 5051.

(19) Graul, S. T.; Squires, R. R. *J. Am. Chem. Soc.* **1988**, *110*, 607.

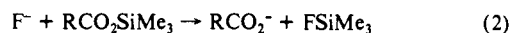
[†] Present address: Department of Chemistry, University of California, Santa Barbara, CA 93106.

expand the scope of the study by including dissociation results for alkoxides²⁰⁻²³ and ketone enolates,²⁴⁻²⁸ as well as for a number of activated endothermic bimolecular reactions. Where the unimolecular dissociations and bimolecular reactions proceed with activation energies that reflect reaction enthalpies, gas-phase acidities can be derived from the measured reaction threshold energies.¹⁹ Conversely, reactions that display activation energies greater or less than the reaction endothermicity can yield useful information about the activated unimolecular reactions of the precursor ions. Thus, the present study has a 2-fold goal: to utilize activated reactions in order to estimate thermochemical properties of carbanions and to examine the characteristics of these activated reactions.

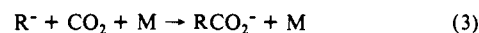
Experimental Section

The apparatus used for these experiments consists of a flowing afterglow ion reactor equipped with a triple quadrupole mass analyzer; the instrument has been described previously.^{14,29} Standard operating conditions in the helium flow reactor were as follows: $P(\text{He}) = 0.3\text{--}0.4$ Torr; buffer gas flow rate, 130–190 STP cm^3/s ; $T = 298 \pm 3$ K. Appearance energies were measured for ionic products from several activated unimolecular decompositions and bimolecular reactions taking place in the gas-tight, rf-only quadrupole collision cell (Q2) of the triple quadrupole analyzer. For these measurements, the ions were produced in the flow tube by the methods described below and mass-selected at the first quadrupole (Q1). Quantitative measurements were carried out at single-collision conditions in Q2 ($P_{\text{Q2}} \leq 5 \times 10^{-5}$ Torr).¹⁶ Unimolecular decompositions were activated by collisions with argon and translationally driven endothermic bimolecular reactions were carried out with the neutral reactant used as the collision gas. Unit-mass resolution (base-line separation of adjacent ion signals) was maintained at the ion-selection quadrupole (Q1) to prevent contamination of the reactant ion by neighboring (± 1 amu) ions. The appearance energies were measured by monitoring the intensity of the product ion as a function of the Q2 dc offset potential, which is taken as the laboratory collision energy.

Ion Production. Primary reagent ions (F^- , OH^- , NH_2^-) were prepared in the ion source region of the flow reactor by electron ionization and ion-molecule reactions.³⁰ Amide ion NH_2^- was formed from NH_3 , hydroxide ion OH^- from a mixture of N_2O and CH_4 (1–2 mTorr), fluoride ion by dissociative electron attachment to SF_6 or CF_4 , and chloride ion by dissociative electron attachment to CCl_4 . Most of the carboxylate ions were prepared by fluorodesilylation of the trimethylsilyl esters (eq 2), as described previously.^{14,16,19} The trimethylsilyl esters were



prepared by mixing the carboxylic acid with a derivatizing agent, bis-(trimethylsilyl)acetamide, and connecting the vial containing the crude reaction mixture directly to the flow tube. Three of the carboxylate ions discussed herein were synthesized in situ by termolecular addition of the carbanion to CO_2 in the flow tube (eq 3).¹⁷ The benzoate ion $\text{C}_6\text{H}_5\text{CO}_2^-$,

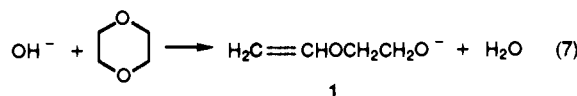
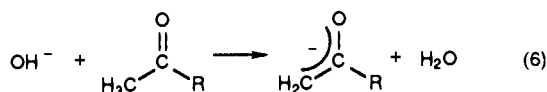


phenylacetate ion $\text{C}_6\text{H}_5\text{CH}_2\text{CO}_2^-$, and cyanoacetate ion $\text{NCCH}_2\text{CO}_2^-$ were synthesized by reaction 3. Phenylacetate ion was also produced by fluorodesilylation of (trimethylsilyl)phenylacetate (eq 2, $\text{R} = \text{C}_6\text{H}_5$) and the cyanoacetate ion was prepared by base-induced elimination of ethylene from the ethyl ester (eq 4). Essentially identical results were



obtained upon collision-induced dissociation (CID) of the ions that were formed by different methods, verifying that the same species is formed in each case.

Most of the alkoxide and ketone enolate ions were prepared by deprotonation of the conjugate acids (eqs 5 and 6). The 2-(vinyl)oxyethoxide ion 1 was generated by an OH^- -induced elimination with 1,4-dioxane (eq 7).³¹



The bimolecular reactions studied included proton abstraction from ethylene and fluoromethane and nucleophilic substitution reactions of Cl^- with $\text{Me}_3\text{SiCH}=\text{CH}_2$ and $\text{Me}_3\text{SiC}_6\text{H}_5$. For these experiments, the reactant ion was generated in the flow tube by one of the methods outlined above, and the neutral reactant was used in the collision quadrupole as the target gas.

Data Analysis. The experimentally determined value of interest for the present study is the threshold energy for an activated unimolecular or bimolecular reaction, E_T . To determine E_T for a unimolecular decomposition or bimolecular reaction, the appearance curve of the reaction product ion is collected by monitoring the intensity of the ionic product as a function of reactant ion axial kinetic energy. Translational energies in the laboratory frame of reference E_{lab} are converted to energies in the center of mass (c.m.) reference frame $E_{\text{c.m.}}$ by eq 8, where M and m are the masses of the reactant ion and the neutral target gas, respectively.

$$E_{\text{c.m.}} = E_{\text{lab}} m / (M + m) \quad (8)$$

The effective center of mass collision energy corresponding to a nominal kinetic energy of the reactant ion is in fact a distribution of collision energies as a result of the reactant ion energy spread and thermal motion of the collision gas. The axial kinetic energy distribution of the reactant ions can be measured by scanning the dc offset potential of the collision quadrupole (Q2) through the nominal ion energy zero (Q2 pole offset = 0 V) and monitoring the reactant ion intensity. The derivative of this cutoff curve yields an approximate reactant ion kinetic energy distribution. For the present experiments, the width of the derivative curve was typically 1–2 eV (fwhm) in the laboratory frame, and the apparent center (the maximum of the derivative curve) was usually within 0.2–0.3 eV (lab) of the nominal ion energy zero. However, the derivative curve was often asymmetric such that the true center could not be easily determined. The small deviations observed (0.2–0.3 eV lab) for the offset of the maximum of the derivative curve translate to even smaller corrections in the center of mass frame (0.05–0.1 eV) and therefore were neglected. Because of the asymmetry and some tailing on the high-energy side, the energy distributions were not well-represented by simple Gaussian (or Lorentzian) functions. In general, the optimized values of E_T are far more sensitive to the choice of the form of the excitation function used to model the data (see below) than to the width of the reactant ion energy distribution. For this reason, and because we suspect that instrumental artifacts contribute to some distortion of the observed reactant ion energy distribution, we approximated the ion energy spread by a Gaussian distribution of 2 eV fwhm for most of the ions. Threshold broadening due to thermal motion of the target gas, also referred to as Doppler broad-

(31) DePuy, C. H.; Bierbaum, V. M. *J. Am. Chem. Soc.* **1981**, *103*, 5034.

(20) (a) Boand, G.; Houriet, R.; Gaumann, T. *Adv. Mass Spectrom.* **1979**, *8A* 238. (b) Houriet, R.; Stahl, D.; Winkler, R. *J. EHP, Environ. Health Perspect.* **1980**, *36*, 63. (c) Boand, G.; Houriet, R.; Gaumann, T. *Lect. Notes Chem.* **1982**, *31*, 195.

(21) (a) Tumas, W.; Foster, R. F.; Pellerite, M. J.; Brauman, J. I. *J. Am. Chem. Soc.* **1983**, *105*, 7464. (b) Tumas, W.; Foster, R. F.; Pellerite, M. J.; Brauman, J. I. *J. Am. Chem. Soc.* **1987**, *109*, 961. (c) Tumas, W.; Foster, R. F.; Brauman, J. I. *J. Am. Chem. Soc.* **1988**, *110*, 2714.

(22) (a) Hayes, R. N.; Sheldon, J. C.; Bowie, J. H.; Lewis, D. E. *J. Chem. Soc., Chem. Commun.* **1984**, 1431. (b) Hayes, R. N.; Sheldon, J. C.; Bowie, J. H.; Lewis, D. E. *Aust. J. Chem.* **1985**, *38*, 1197.

(23) Sulzle, D.; Schwarz, H. *Helv. Chim. Acta* **1989**, *72*, 320.

(24) Stringer, M. B.; Bowie, J. H.; Holmes, J. L. *J. Am. Chem. Soc.* **1986**, *108*, 3888.

(25) (a) Hunt, D. F.; Shabanowitz, J.; Giordani, A. B. *Anal. Chem.* **1980**, *82*, 386. (b) Hunt, D. F.; Giordani, A. B.; Shabanowitz, J.; Rhodes, G. *J. Org. Chem.* **1982**, *47*, 738.

(26) (a) Moylan, C. R.; Jasinski, J. M.; Brauman, J. I. *Chem. Phys. Lett.* **1983**, *98*, 1. (b) Foster, R. F.; Tumas, W.; Brauman, J. I. *J. Chem. Phys.* **1983**, *79*, 4644. (c) Moylan, C. R.; Jasinski, J. M.; Brauman, J. I. *J. Am. Chem. Soc.* **1985**, *107*, 1934.

(27) (a) Stringer, M. B.; Underwood, D. J.; Bowie, J. H.; Holmes, J. L.; Mommers, A. A.; Szulejko, J. A. *Can. J. Chem.* **1986**, *63*, 764. (b) Stringer, M. B.; Bowie, J. H.; Holmes, J. L. *J. Am. Chem. Soc.* **1986**, *108*, 3888. (c) Bowie, J. H.; Stringer, M. B.; Currie, G. J. *J. Chem. Soc., Perkin Trans. 2* **1986**, 2, 1821. (d) Hayes, R. N.; Sheldon, J. C.; Bowie, J. H. *Int. J. Mass Spectrom. Ion Processes* **1986**, *71*, 233. (e) Currie, G. J.; Stringer, M. B.; Bowie, J. H.; Holmes, J. L. *Aust. J. Chem.* **1987**, *40*, 1365. (f) Raftery, M. J.; Bowie, J. H. *Int. J. Mass Spectrom. Ion Processes* **1987**, *79*, 207. (g) Raftery, M. J.; Bowie, J. H. *Aust. J. Chem.* **1985**, *20*, 4.

(28) (a) Young, A. B.; Harrison, A. G. *Org. Mass Spectrom.* **1987**, *22*, 622. (b) Donnelly, A.; Chowdhury, S.; Harrison, A. G. *Org. Mass Spectrom.* **1989**, *24*, 89.

(29) (a) Lane, K. R.; Lee, R. E.; Sallans, L.; Squires, R. R. *J. Am. Chem. Soc.* **1984**, *106*, 5767. (b) Squires, R. R.; Lane, K. R.; Lee, R. E.; Wright, L. G.; Wood, K. V.; Cooks, R. G. *Int. J. Mass Spectrom. Ion Processes* **1985**, *64*, 185. (c) Graul, S. T.; Squires, R. R. *Mass Spectrom. Rev.* **1987**, *7*, 263.

(30) DePuy, C. H.; Bierbaum, V. M. *Acc. Chem. Res.* **1981**, *14*, 146.

ening, was treated according to the model developed by Chantry.³²

In the low-pressure limit, the intensity of a product ion is related to the energy-dependent reaction cross section by eq 9, where I_P and I_R are

$$\ln \left(\frac{I_P}{I_0} \right) \sim \frac{I_P}{I_0}(E) = \frac{I_P}{I_R + \sum I_P}(E) = \sigma_P(E)nl \quad (9)$$

the intensities of the product and reactant ions, respectively, I_0 is the total ion intensity ($I_0 = I_R + \sum I_P$; $I_P \ll I_0$), $\sigma_P(E)$ is the observed cross section for the reaction at energy E , n is the collision gas number density, and l is the effective path length. The energy dependence of the reaction cross section can be modeled by using the excitation function shown in eq 10,³³ where σ_0 is a scaling factor, E is the center of mass translational energy of the reactants, E_T is the activation energy for the reaction, and n and m are adjustable parameters.

$$\sigma_P(E) = \sigma_0 \frac{(E - E_T)^n}{E^m} \quad (10)$$

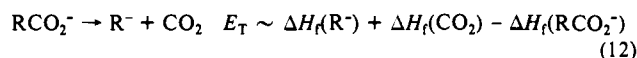
In the quadrupole collision cell, the transmission characteristics of the parent or reactant ion and the fragment(s) or product ion(s) are very different. A commonly observed artifact of the differing transmission is an oscillatory pattern in the reactant ion absolute intensity when monitored as a function of axial kinetic energy.^{34,35} This pattern is not reproduced in the product ion appearance curve, which typically rises smoothly above threshold to a maximum product ion yield. The oscillatory pattern observed for the reactant ion prevents accurate measurements of the reactant ion intensity, which is a quantity required for the calculation of reaction cross sections. However, this limitation does not preclude the determination of reaction threshold energies (E_T), which are the quantities of interest for the present study. Examination of the reactant ion transmission function at retarding to low attractive voltages at the collision cell indicates that the reactant ion intensity usually attains the approximate maximum value at 1–3 eV axial kinetic energy in the laboratory frame of reference. These values typically correspond to much smaller relative translational energies in the center of mass frame of reference. From the observation of smoothly rising appearance curves for product ions, it seems safe to assume that the reactant ion intensity incident on the collision cell is essentially constant above ~ 2 eV lab. Although the effective path length through the collision cell is also energy-dependent,³⁶ the path length at axial kinetic energies above a few electronvolts lab does not change significantly. Thus, eq 9 can be rearranged to give eq 11, with the assumption that the effective path length

$$\frac{I_P(E)}{I_P(\max)} = \frac{\sigma_P(E)I_0nl}{I_P(\max)} = \frac{\sigma_0 I_0 nl}{I_P(\max)} \frac{(E - E_T)^n}{E^m} = \sigma_0' \frac{(E - E_T)^n}{E^m} \quad (11)$$

and the total ion intensity can be taken as constant. The raw ion intensity is normalized to the maximum yield $I_P(\max)$. The factors $[\sigma_0 I_0 nl / I_P(\max)]$ are combined to give an effective scaling factor of σ_0' . Within the above assumptions, the appearance curves for product ions can be modeled by an excitation function of the same general form as that often used to model reaction cross sections. Convolved into the trial appearance curves calculated by use of eq 11 are contributions to threshold broadening from the kinetic energy spread of the reactant ion and from the thermal motion of the target gas.^{37,38} The trial curves are fit to the experimental data by an iterative procedure in which any or all of the parameters in eq 11 (i.e., σ_0' , E_T , n , and m) can be varied until the fit is optimized.

Threshold behavior for endothermic reactions and activated unimolecular decompositions is not well-understood, particularly when polyatomic species are involved. The values of n and m that have been used in the excitation function (eq 10) for analysis of experimental data^{37–44}

or predicted by theory^{33,45–48} vary widely, and it is not clear what would be an appropriate choice for the present study. Because we cannot predict a priori what the appropriate values of n and m should be for all the reactions under investigation, we have adopted an empirical approach to the data analysis. Simple linear fits of the experimental data indicate that the measured threshold energies for CO_2 loss from the carboxylate ions correspond approximately to the enthalpies of reaction 12 for ground



state, thermal energy reactants, and products. This observation is consistent with the expected lack of a barrier in excess of the heterolytic bond energy^{17,18} and further indicates that there are not substantial kinetic shifts resulting from slow dissociations.

To optimize the parameters in eq 11 for the data analysis, we selected as reference systems several carboxylate ions for which the values of $\Delta H_f(\text{R}^-)$ and $\Delta H_f(\text{RCO}_2^-)$ were known independently. The decarboxylation threshold data for these systems were then used to determine which values of n and m yielded both satisfactory fits to the experimental data and values of E_T that were in accord with eq 12. The reference carboxylates chosen were CF_3CO_2^- , $\text{C}_6\text{H}_5\text{CO}_2^-$, $\text{NCCH}_2\text{CO}_2^-$, and CH_3CO_2^- . Trial appearance curves were calculated by using eq 11 with an initial value of E_T derived from eq 12 and various values of n and m . Broadening caused by the energy distribution of the reactant ion and the thermal motion of the target gas was accounted for by convoluting these contributions into the calculated curves, which were then iteratively fit to the experimental data by optimizing the scaling constant (σ_0' in eq 11) and the value of E_T . Values for the parameters n and m between 0 and 3 were considered, and several sets were found to yield qualitatively good fits to the experimental data.³⁸ The best agreement between the optimized values of E_T and the thermochemical value (eq 12) with acceptable fits to the data was obtained in trial curves that were calculated by using eq 11 with $n = m = 1.5$ and $n = 1$, $m = 0.5$. These two sets of parameters were used to calculate product ion appearance curves for each of the CID processes examined.

Some of the experimental appearance curves displayed a slow rise leading to the apparent threshold region. This "tailing" behavior was affected by instrumental settings such as the tuning at the lenses in the ion sampling region, whereas the nominal threshold energy given by a simple linear fit of the steeply rising portion of the appearance curve was usually unperturbed.^{16,19} Full optimization of the calculated appearance curves, varying n and m as well as E_T and the scaling constant σ_0' to fit the entire threshold region, resulted in extremely large values of n and m (up to 25) and yielded absurdly low values of E_T . The tailing that we observe in the threshold region is probably at least in part an artifact of the method used to sample ions from the flow tube; collisional activation in the local high-pressure zone behind the sampling orifice can cause elevated internal energy in some fraction of the reactant ions, leading to their fragmentation in Q2 at collision energies below the threshold for dissociation of thermal energy ions. In general, the calculated appearance curves were optimized by weighting most heavily the steeply rising portion of the experimental curve.

The appearance curves for the bimolecular reactions examined were also treated with the $n = m = 1.5$ and $n = 1$, $m = 0.5$ models, which generally fit the data quite well. For the light ion OH^- , the kinetic energy distributions of the reactant ions were somewhat narrower (1–1.5 eV lab) than for the heavier ions. The trial appearance curves for these data were therefore convoluted with Gaussian ion energy distribution of 1.5 eV fwhm.

Results

Carboxylate Ions. Low-energy CID of many carboxylate ions RCO_2^- results in production of R^- by decarboxylation.¹⁹ In the preceding paper in this issue,¹⁴ we described in detail the processes observed upon collisional activation of aliphatic, unsaturated, and

(32) Chantry, P. J. *J. Chem. Phys.* **1971**, *55*, 2746.

(33) Levine, R. D.; Bernstein, R. B. *Molecular Reaction Dynamics*; Oxford University Press: New York, 1974; Chapter 2.

(34) Dawson, P. H., Ed. *Quadrupole Mass Spectrometry and Its Applications*; Elsevier: New York, 1976.

(35) Miller, P. E.; Bonner Denton, M. *Int. J. Mass Spectrom. Ion Processes* **1986**, *72*, 223.

(36) Dawson, P. H.; Fulford, J. L. *Int. J. Mass Spectrom. Ion Phys.* **1982**, *42*, 195.

(37) Lifshitz, C.; Wu, R. L. C.; Tiernan, T. O.; Terwiliger, D. T. *J. Chem. Phys.* **1978**, *68*, 247.

(38) (a) Ervin, K. M.; Armentrout, P. B. *J. Chem. Phys.* **1985**, *83*, 166.

(b) Aristov, N.; Armentrout, P. B. *J. Am. Chem. Soc.* **1986**, *108*, 1806.

(39) Hopper, D. G.; Wahl, A. C.; Wu, R. L. C.; Tiernan, T. O. *J. Chem. Phys.* **1976**, *65*, 5474.

(40) Berkowitz, J.; Chupka, W. A.; Gutman, D. *J. Chem. Phys.* **1971**, *55*, 2733.

(41) Frobin, W.; Schlier, Ch.; Stein, K.; Teloy, E. *J. Chem. Phys.* **1977**, *67*, 5505.

(42) Armentrout, P. B.; Beauchamp, J. L. *J. Chem. Phys.* **1981**, *74*, 2819.

(43) Jarrold, M. F.; Bower, J. E. *J. Am. Chem. Soc.* **1988**, *110*, 70.

(44) Hanley, L.; Ruatta, S. A.; Anderson, S. L. *J. Chem. Phys.* **1987**, *87*, 260.

(45) Morokuma, K.; Eu, B. C.; Karplus, M. *J. Chem. Phys.* **1969**, *51*, 5193.

(46) Eu, B. C.; Liu, W. S. *J. Chem. Phys.* **1975**, *63*, 592.

(47) Menzinger, M.; Yokozeki, A. *Chem. Phys.* **1977**, *22*, 273.

(48) (a) Chesnavich, W. J.; Bowers, M. T. *J. Chem. Phys.* **1978**, *68*, 901.

(b) Chesnavich, W. J.; Bowers, M. T. *J. Phys. Chem.* **1979**, *83*, 900.

Table I. Decarboxylation Threshold Energies and Thermochemistry for Reference Ions^a

RCO ₂ ⁻	R ⁻	E _T ^b	ΔH _f (RCO ₂ ⁻) ^c	ΔH _f (R ⁻) ^c	ΔH _{rxn} ^d
CF ₃ CO ₂ ⁻	CF ₃ ⁻	40.1 ± 4.6 (1.74 ± 0.20)	-289.2 ± 4.3	-154.9 ± 2.4	40.3 ± 4.3
CH ₃ CO ₂ ⁻	CH ₃ ⁻	61.6 ± 3.5 (2.67 ± 0.15)	-120.4 ± 3.1	33.2 ± 1.9	59.6 ± 3.1
NCCH ₂ CO ₂ ⁻	NCCH ₂ ⁻	34.1 ± 4.6 (1.48 ± 0.20)	-106.4 ± 7.6	25.1 ± 2.9	37.5 ± 7.6
C ₆ H ₅ CO ₂ ⁻	C ₆ H ₅ ⁻	60.6 ± 3.5 (2.63 ± 0.15)	-97.3 ± 3.3	54.7 ± 0.7	58.0 ± 3.3

^aAll values in kilocalories per mole. ^bValues in parentheses are E_T in eV. Uncertainties are 2 standard deviations or 0.15 eV, whichever is larger. ^cAll data taken from ref 7. ^dΔH_{rxn} = ΔH_f(R⁻) + ΔH_f(CO₂) - ΔH_f(RCO₂⁻); ΔH_f(CO₂) = -94.05 kcal/mol; ref 7.

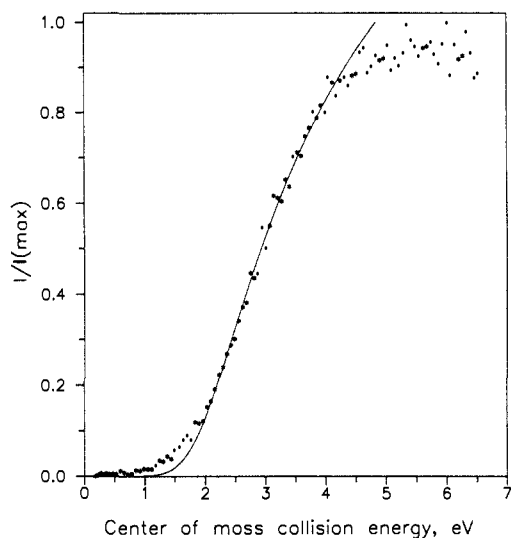


Figure 1. Appearance curve for CF₃⁻ from decarboxylation of CF₃CO₂⁻ by collisions with argon gas at 5 × 10⁻⁵ Torr. The solid line is the optimized model appearance curve calculated with eq 10 and n = m = 1.5.

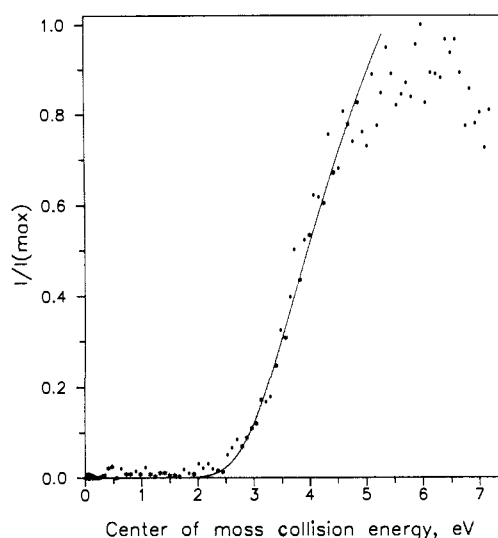


Figure 2. Appearance curve for 1-methylcyclopropyl anion from decarboxylation of 1-methylcyclopropanecarboxylate anion by collisions with argon gas at 5 × 10⁻⁵ Torr. The solid line is the optimized model appearance curve calculated with eq 10 and n = m = 1.5.

saturated carboxylate ions (see also refs 49–52). Decarboxylation appears to be a universal fragmentation pathway for carboxylate ions and is usually the lowest energy decomposition route observed. In many cases, the carbanions formed by decarboxylation are the exclusive CID products observed for collision energies below ~5 eV c.m.¹⁴

Appearance energy measurements were made for the carbanions produced by CID of a series of over 20 different carboxylate ions. The experimental data from CF₃CO₂⁻, NCCH₂CO₂⁻, C₆H₅CO₂⁻, and CH₃CO₂⁻ were used to optimize the choice of parameters n and m in the cross-section function (eq 11) used to fit the data. Heats of formation for RCO₂⁻ and R⁻ are known for these species and therefore the enthalpy changes for decarboxylation are known. If, upon collisional activation, decarboxylation proceeds rapidly and without a barrier in the exit channel, then the measured threshold energy should reflect the enthalpy of decarboxylation. To optimize the parameters used in the excitation function for the present analyses (eq 11), trial appearance curves were calculated for each of the reference carboxylates with various values of n and m and values of E_T derived from eq 12. The calculated curves were convoluted with the reactant ion energy spread and

the Doppler broadening contribution from the motion of the target gas.^{32,37,38} With n and m held constant, E_T and the scaling constant σ₀' were varied to optimize the fit of the calculated curve to the experimental data. Parameters n and m were selected for analysis of the data on the basis of the quality of the fit of the calculated curves to the experimental data and the agreement of the optimized value of E_T with the predicted enthalpy of decarboxylation of the reference ions. The parameters chosen for calculation of the trial appearance curves for the present study are n = m = 1.5 and n = 1, m = 0.5 (eq 11). These values are similar to those used in several studies in the literature.^{37–43}

Shown in Figure 1 is a set of experimental data for decarboxylation of CF₃CO₂⁻ and the convoluted excitation function with n = m = 1.5. The optimized fit is satisfactory over most of the rise, and the resulting value of E_T (1.70 eV or 39.2 kcal/mol) is in excellent agreement with the enthalpy of decarboxylation of CF₃CO₂⁻ (ΔH = 40.4 kcal/mol or 1.75 eV).⁷ In Table I, the values of E_T from the optimized excitation functions are listed for the reference carboxylate ions. The threshold energies given are the averages of the values given by the model with n = m = 1.5 and with n = 1, m = 0.5 for at least three replicate measurements. The uncertainty quoted is twice the standard deviation or 0.15 eV, whichever is larger, and reflects both the reproducibility of the data and the differences in E_T given by the two excitation functions. Also listed are the decarboxylation enthalpies derived from accepted literature values for ΔH_f(RCO₂⁻) and ΔH_f(R⁻). The agreement between the measured threshold energies and the enthalpy of decarboxylation is within the experimental error for all the reference systems.

The experimental appearance curve for each of the carboxylates was modeled with both the n = m = 1.5 and n = 1, m = 0.5 parameter sets, and the threshold energy E_T and scaling factor σ₀' were optimized for best fit. The quality of the fit was best for appearance curves that showed the least broadening in the threshold region. An example of such a data set is shown in Figure

(49) Stringer, M. B.; Bowie, J. H.; Eichinger, P. C. H.; Currie, G. *J. Chem. Soc., Perkin Trans. 2* **1987**, 385.

(50) (a) Tomer, K. B.; Crow, F. W.; Gross, M. L. *J. Am. Chem. Soc.* **1983**, *105*, 5487. (b) Jensen, N. J.; Tomer, K. B.; Gross, M. L. *Anal. Chem.* **1985**, *57*, 2018. (c) Jensen, N. J.; Tomer, K. B.; Gross, M. L. *J. Am. Chem. Soc.* **1985**, *107*, 1863.

(51) (a) Wysocki, V. H.; Bier, M. E.; Cooks, R. G. *Org. Mass Spectrom.* **1988**, *23*, 627. (b) Wysocki, V. H.; Ross, M. M.; Horning, S. R.; Cooks, R. G. *Rapid Commun. Mass Spectrom.* **1988**, *2*, 214.

(52) Aurelle, H.; Treilhou, M.; Prome, D.; Savagnac, A.; Prome, J. C. *Rapid Commun. Mass Spectrom.* **1987**, *1*, 65.

(53) Graul, S. T.; Schnute, M. E.; Squires, R. R., submitted for publication in *Int. J. Mass Spectrom. Ion Processes*.

(54) Benson, S. W. *Thermochemical Kinetics*, 2nd ed.; John Wiley & Sons: New York, 1976.

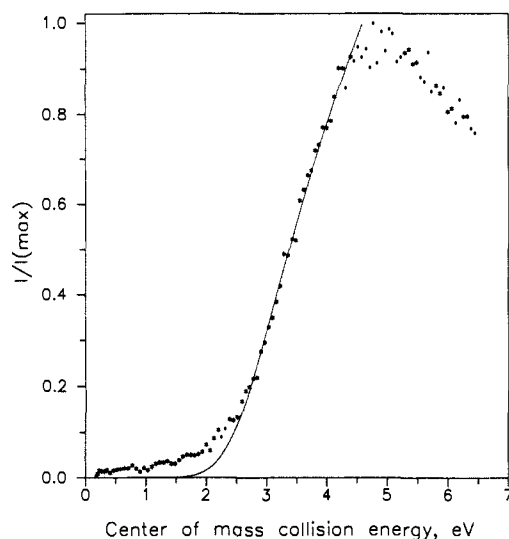


Figure 3. Appearance curve for β -acetyethyl anion from decarboxylation of levulinate anion by collisions with argon gas at 5×10^{-5} Torr. The solid line is the optimized model appearance curve calculated with eq 10 and $n = m = 1.5$.

2, which displays the experimental appearance curve for decarboxylation of 1-methylcyclopropanecarboxylate, along with the curve calculated with the $n = m = 1.5$ model. The maximum observed in the product ion yield is a common feature in the appearance curves for products of decarboxylation. Among the possible causes for this feature are instrumental artifacts such as the decreased observation time scale as the ion axial kinetic energy increases; i.e., activated ions may exit the collision cell before fragmentation occurs. Physical effects that may be involved include changes in the total collision cross section or in the decarboxylation cross section. Chemical processes such as electron detachment from or further fragmentation of the product ions may also be occurring, perhaps in combination with the other factors suggested above. Because of the ambiguity regarding the cause for these features, no attempt was made to fit the high-energy part of the appearance curve.

In some of the experimental data, broadening (tailing) was apparent in the threshold region. An example of such data is shown in Figure 3, which shows the appearance curve for the product of decarboxylation of levulinate ion $\text{CH}_3\text{C}(\text{O})\text{CH}_2\text{C}-\text{H}_2\text{CO}_2^-$. The fit obtained by optimizing to the steeply rising portion is good for most of the data up to the maximum, but does not reproduce the broadness in the threshold region. In some extreme cases, the broadening results in a slow rise in product ion intensity, starting near 0 eV c.m. and continuing up to the apparent threshold (i.e., the region of a steepest rise, e.g., Figure 4). Analysis of the initial rise in such data results in threshold energies for decarboxylation of 0–0.5 eV, which is unreasonable for thermal energy carboxylate ions of this nature. Moreover, such analyses do not reproduce the steeply rising portion of the appearance curve when the parameters n and m are held between 0 and 3. It is not clear what causes the broadening in particular appearance curves to be (reproducibly) worse than that observed for the other carboxylates mentioned above. However, it is interesting to note that a common feature of the carboxylates that display this type of behavior is unsaturation in the α position. For example, the α,β -unsaturated carboxylates $\text{CH}_3\text{CH}=\text{CHCO}_2^-$ and $\text{CH}_2=\text{C}(\text{CH}_3)\text{CO}_2^-$ and the α -carbonyl carboxylate $\text{CH}_3\text{C}(\text{O})\text{CO}_2^-$ all yield broadened appearance curves for their decarboxylation products. It is possible that such species are particularly sensitive to collisional excitation in the sampling region or require the use of different forms of the excitation function. A further possibility (to be discussed in more detail in the Discussion) is partial isomerization either of the parent carboxylate ion or of the nascent product ion within the dissociating complex, such that a mixture of product ions is formed and an admixture of appearance curves with different true threshold energies is obtained. Note that for the observed threshold energy to be affected, any

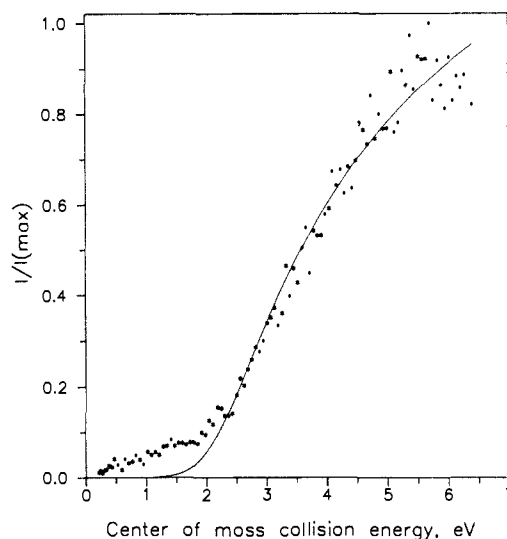
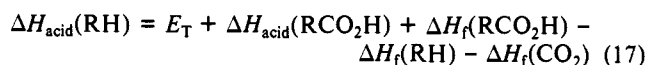
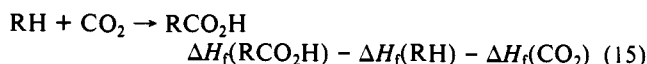
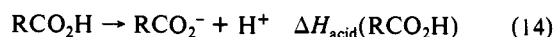


Figure 4. Appearance curve for 1-propenyl anion from decarboxylation of $\text{CH}_3\text{CH}=\text{CHCO}_2^-$ by collisions with argon gas at 5×10^{-5} Torr. The solid line is the optimized model appearance curve calculated with eq 10 and $n = m = 1.5$.

isomerization of the product ion must occur prior to its departure from the dissociating complex, and the isomerization must have a lower activation energy than that for CO_2 loss; this activation method is obviously blind to any unimolecular rearrangements of the isolated product ions once they are formed.

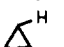


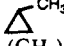

By relating the measured threshold energy for decarboxylation of RCO_2^- to the overall enthalpy of reaction 12, it is possible to derive gas-phase acidities for the conjugate acids (RH) of the carbanions (R^-) produced. Through the use of the thermochemical cycle shown in eqs 13–17, a value for $\Delta H_{\text{acid}}(\text{RH})$ can be derived from the measured decarboxylation threshold energy and available literature values for the heat of formation and acidity of RCO_2H .



The gas-phase acidities derived by use of eq 17 for the decarboxylation results are given in Table II, along with the thermochemical data used. Where literature values of $\Delta H_{\text{acid}}(\text{RH})$ are available, they are included for comparison. The uncertainty for $\Delta H_{\text{acid}}(\text{RH})$ calculated from the decarboxylation threshold energy is taken as the maximum uncertainty associated with any individual value used in eq 17. Strictly speaking, the values of $\Delta H_{\text{acid}}(\text{RH})$ derived from the decarboxylation results should represent upper limits to the true $\Delta H_{\text{acid}}(\text{RH})$. However, these values obtained for at least six of the RH species seem unreasonably low. Indeed, the value of $\Delta H_{\text{acid}}(\text{CH}_3\text{CH}_2\text{CH}=\text{CH}_2)$ given by the decarboxylation results (381 ± 3.5 kcal/mol) is lower than would be expected for any hydrogen in 1-butene, and our value for $\Delta H_{\text{acid}}[(\text{CH}_2)\text{CHCH}_3]$ (390 ± 5 kcal/mol) is also unreasonably low. Plausible explanations for these anomalies include isomerization of the parent carboxylate, excitation in the sampling region, and impurity species in the parent ion population; these possibilities are considered in more depth in the Discussion, where we also analyze results for the other reactive systems described below.

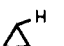
For almost all the carboxylate ions listed in Table II, decarboxylation is the lowest energy fragmentation pathway observed to occur. One exception is $\text{CF}_3\text{CH}_2\text{CH}_2\text{CO}_2^-$, which loses HF as the lowest energy process with a measured threshold energy of 1.73 ± 0.15 eV. Loss of HF probably occurs by an initial

Table II. Upper Limit for $\Delta H_{\text{acid}}(\text{RH})$ Derived from the Threshold Decarboxylation Energy of RCO_2^-

RH	E_T , eV	$\Delta H_f(\text{RCO}_2\text{H})^a$	$\Delta H_{\text{acid}}(\text{RCO}_2\text{H})^a$	$\Delta H_f(\text{RH})^a$	$\Delta H_{\text{acid}}(\text{RH})$	
					this study	lit. ^a
CF_3H	1.74 ± 0.20	-246.4 ± 0.2	322.7 ± 4	-166 ± 0.5	376 ± 4.5	377 ± 2
CF_2H_2	2.31 ± 0.16	-197 ± 4	330.8 ± 3	-108 ± 0.5	389 ± 3.5	387 ± 7
CFH_3	2.55 ± 0.22	-140 ± 2	338.4 ± 3	-59	410 ± 4.5	
CH_4	2.67 ± 0.15	-103.3 ± 0.1	348.7 ± 3	-17.8 ± 0.1	418.8 ± 3.5	416.8 ± 1.7
CH_3CN	1.48 ± 0.20	-71 ± 5	330.3 ± 3	18.0 ± 0.2	369 ± 4.5	373 ± 26
C_2H_4	2.59 ± 0.15	-77	344 ± 3 ^b	12.5 ± 0.2	408 ± 3.5	407.5 ^d
CH_2CHO	1.84 ± 0.15	-131	334 ± 4 ^b	-39.6 ± 0.1	379 ± 3.5	391 ± 2.6
$\text{CF}_3\text{CH}_2\text{CH}_3$	2.74 ± 0.16	-264 ^c	337 ± 4 ^b	-176 ^c	406 ± 3.5	
	2.58 ± 0.20	-78	346 ± 3 ^b	12.7 ± 0.2	409 ± 4.5	411.5 ^d
$\text{CH}_3\text{CH}=\text{CH}_2$	1.97 ± 0.15	-84	344 ± 3 ^b	4.8 ± 0.2	395 ± 3.5	>405 ^e
$\text{CH}_3\text{CH}=\text{CH}_2$	2.20 ± 0.25	-88	343 ± 3 ^b	4.8 ± 0.2	395 ± 5	405.8 ^d
	2.73 ± 0.16	-84 ^c	346 ± 3 ^b	5.5	413 ± 3.7	
	2.68 ± 0.34	-84 ^c	344 ± 3 ^b	5.5	411 ± 7	409.2 ^d
	1.81 ± 0.25	-84 ^c	345 ± 3 ^b	5.5	391 ± 6	410.5 ^d
$(\text{CH}_3)_2\text{C}=\text{CH}_2$	2.00 ± 0.16	-98	345 ± 3 ^b	-4.0 ± 0.1	391 ± 3.7	
$\text{CH}_2=\text{CHCH}_2\text{CH}_3$	1.34 ± 0.15	-88 ^c	344 ± 3 ^b	-0.1 ± 0.1	381 ± 3.5	
$\text{CH}_2=\text{CHCH}_2\text{CH}_3$	2.54 ± 0.16	-90	343 ± 3 ^b	-0.1 ± 0.1	408 ± 3.7	
$\text{CH}_3\text{C}(\text{O})\text{CH}_2\text{CH}_3$	2.32 ± 0.18	-145 ^c	341 ± 3 ^b	-57.5 ± 0.1	401 ± 4.0	
	2.73 ± 0.15	-38.8 ^c	345 ± 3 ^b	49.7	411 ± 3.5	
$\text{C}(\text{CH}_3)_4$	2.90 ± 0.15	-128.6 ± 1	345 ± 2.5	-40.0 ± 0.1	417 ± 3.5	408.9 ^d
C_6H_6	2.63 ± 0.15	-70.3 ± 0.5	339 ± 3	19.8 ± 0.1	403 ± 3.5	400.8 ± 0.5
$\text{CH}_2=\text{CHC}(\text{CH}_3)_3$	2.62 ± 0.18	-102 ^c	342 ± 3 ^b	-14.5 ± 0.2	409 ± 4	
$\text{C}_6\text{H}_5\text{CH}_3$	1.28 ± 0.15	-76 ± 1	341 ± 2.6	12.0 ± 0.1	377 ± 3.5	381 ± 2.5

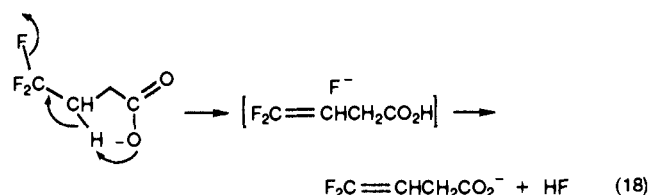
^a Reference 7 unless otherwise indicated; all values in kilocalories per mole; uncertainties taken from ref 7. ^b Reference 53. ^c Estimated by use of group increments; ref 54. ^d Reference 13b. ^e Reference 15.

Table III. Upper Limits for $\Delta H_{\text{acid}}(\text{RH})$ Derived from Threshold Energies for CID of Alkoxides

RH	ROH	E_T , eV	$\Delta H_f(\text{ROH})^a$	$\Delta H_{\text{acid}}(\text{ROH})^a$	$\Delta H_f(\text{RH})^a$	$\Delta H_{\text{acid}}(\text{RH})$	
						this study	lit. ^a
CH_4	$\text{CH}_3\text{CH}_2\text{OH}$	2.17 ± 0.16	-56.2 ± 0.1	377.4 ± 2.4	-17.8 ± 0.1	415 ± 3.7	416.8 ± 1.7
	$(\text{CH}_3)_2\text{CHOH}$	2.32 ± 0.16	-65.2 ± 0.1	375.5 ± 2.4	-17.8 ± 0.1	421 ± 3.7	
CH_3F	$\text{FCH}_2\text{CH}_2\text{OH}$	3.09 ± 0.27	-100 ± 2	370.0 ± 4	-59	427 ± 6.2	
C_2H_4	$\text{CH}_2=\text{CHCH}_2\text{OH}$	2.08 ± 0.40	-30 ± 0.5	373 ± 3 ^c	12.5 ± 0.2	405 ± 9.2	407.5 ^d
	$(\text{CH}_2)_2\text{CHCH}_2\text{OH}$	2.22 ± 0.26	-31 ^b	374 ± 3 ^c	12.7 ± 0.2	407 ± 6.0	411.5 ^d
$\text{CH}_3\text{CH}=\text{CH}_2$	$\text{CH}_3\text{CH}=\text{CH}_2\text{CH}_2\text{OH}$	1.82 ± 0.22	-37 ± 1	374 ± 3 ^c	4.8 ± 0.2	400 ± 5.1	>405 ^e
$\text{CH}_2=\text{CHOCH}_3$	$\text{CH}_2=\text{CHOCH}_2\text{CH}_2\text{OH}$	2.68 ± 0.52	-70 ^b	369 ± 3 ^c	-24 ± 2	411 ± 12	
$\text{C}(\text{CH}_3)_4$	$(\text{CH}_3)_3\text{CCH}_2\text{CH}_2\text{OH}$	2.00 ± 0.24	-79.3 ± 1.0	372.6 ± 2.6	-40.0 ± 0.1	405 ± 5.5	408.9 ^d
C_6H_6	$\text{C}_6\text{H}_5\text{CH}_2\text{OH}$	1.66 ± 0.24	-24.0 ± 0.2	370.0 ± 3.0	19.8 ± 0.1	391 ± 5.5	400.8 ± 0.5
	$\text{C}_6\text{H}_5\text{CH}(\text{CH}_3)\text{OH}$	1.87 ± 0.15	-27.1 ^b	368 ^d	19.8 ± 0.1	403 ± 3.5	
$\text{C}_6\text{H}_5\text{CH}_2\text{CH}_3$	$\text{C}_6\text{H}_5\text{CH}_2\text{CH}_2\text{CH}_2\text{OH}$	2.14 ± 0.20	-33.8 ^b	373 ^d	7.0 ± 0.1	406 ± 4.6	

^a Reference 7 unless otherwise indicated. $\Delta H_{\text{acid}}(\text{CH}_2\text{O}) = -26.0 \pm 0.2$ kcal/mol; $\Delta H_f(\text{CH}_3\text{CHO}) = -39.6 \pm 0.1$ kcal/mol. All values in kilocalories per mole. ^b Estimated by use of group increments; ref 54. ^c Reference 53. ^d Reference 13b. ^e Reference 15.

intramolecular proton transfer followed by or simultaneous with loss of F^- , which abstracts the carboxylic proton as it departs:

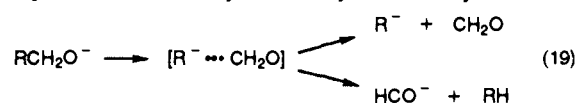


The enthalpy change for this reaction can be estimated by assuming $\Delta H_{\text{acid}}(\text{CF}_2=\text{CHCH}_2\text{CO}_2\text{H}) \sim 340$ kcal/mol [slightly higher than $\Delta H_{\text{acid}}(\text{CF}_3\text{CH}_2\text{CH}_2\text{CO}_2\text{H}) = 336.5 \pm 3.6$ kcal/mol; Table III] and using group increments to estimate $\Delta H_f(\text{CF}_2=\text{CHCH}_2\text{CO}_2\text{H})$ as -166 kcal/mol.⁵⁵ These values yield ΔH_f

(55) $\Delta H_f(\text{CF}_3\text{CH}_3) = -179$ kcal/mol; $\Delta H_f(\text{CF}_2=\text{CH}_2) = -82$ kcal/mol; $\delta\Delta H_f = +97$ kcal/mol. $\Delta H_f(\text{CF}_3\text{CH}=\text{CH}_2) = -147$ kcal/mol; $\Delta H_f(\text{CF}_2=\text{C}=\text{CH}_2) = -48$ kcal/mol; $\delta\Delta H_f = +99$ kcal/mol. $\Delta H_f(\text{CF}_3\text{CH}_2\text{CH}_2\text{CO}_2\text{H}) = -264$ kcal/mol; $\delta\Delta H_f \sim +98$ kcal/mol; $\Delta H_f(\text{CF}_2=\text{CHCH}_2\text{CO}_2\text{H}) = -166$ kcal/mol.

($\text{CF}_2=\text{CHCH}_2\text{CO}_2^-$) ~ -192 kcal/mol and $\Delta H(\text{eq 18}) \sim 37$ kcal/mol or 1.60 eV, in reasonable agreement with the measured threshold energy.

Alkoxide and Ketone Enolate Ions. Low-energy collisional activation of primary alkoxide ions RCH_2O^- leads to formation of R^- and CH_2O . When R^- is a strongly basic ion, proton transfer within the activated complex can also occur, yielding RH and HCO^- (eq 19).²⁰⁻²³ Similarly, secondary and tertiary alkoxides



can dissociate to yield R^- and an aldehyde or ketone, respectively, or the enolate ions and RH if proton transfer occurs. We have measured appearance energies for the R^- product formed by CID of a number of alkoxide ions.

The experimental appearance curves for products from CID of the alkoxide ions were analyzed in the same manner as those of the carboxylate ions. Although some of the data was adequately modeled (for example, CID of allyl alkoxide; Figure 5), several

Table IV. Upper Limits for $\Delta H_{\text{acid}}(\text{RH})$ Derived from Threshold Energies for Production of R^- from $\text{RC}(\text{O}^-)\text{CH}_2$

RH	E_{T} , eV	$\Delta H_{\text{T}}(\text{RCOCH}_3)^a$	$\Delta H_{\text{acid}}(\text{RCOCH}_3)^a$	$\Delta H_{\text{T}}(\text{RH})^a$	$\Delta H_{\text{acid}}(\text{RH})$	
					this study	lit. ^a
C_2H_4	2.81 ± 0.18	-33.0 ± 2.0	363.3 ± 2.6	12.5 ± 0.2	408 ± 4.2	407.5^b
CH_3CHO	2.04 ± 0.14	-78.2 ± 0.3	358 ± 3^c	-39.6 ± 0.1	396 ± 3.5	391 ± 2.6
$\text{CH}_2=\text{CHCH}_2\text{CH}_3$	3.02 ± 0.15	-36.6^d	368^c	-0.1 ± 0.1	393 ± 3.5	412.0^b
C_6H_6	3.39 ± 0.20	-20.7 ± 0.4	361.4 ± 2.6	19.8 ± 0.1	402 ± 4.6	400.8 ± 0.5

^aData taken from ref 7 unless otherwise indicated. All values in kilocalories per mole. ^bReference 13b. ^cReference 53. ^dEstimated from group increments; ref 54.

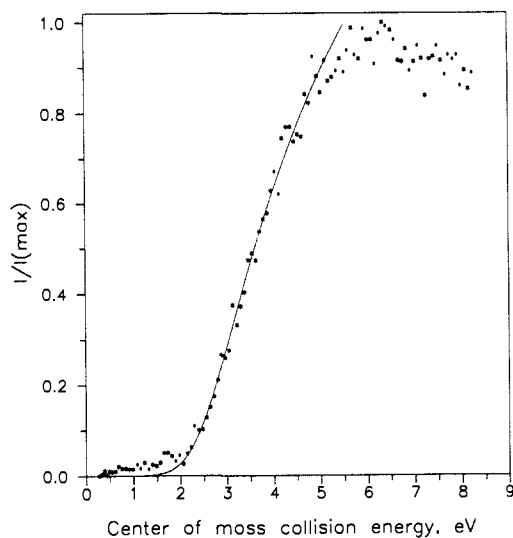


Figure 5. Appearance curve for vinyl anion from CID of allyl alkoxide by collisions with argon gas at 5×10^{-5} Torr. The solid line is the optimized model appearance curve calculated with eq 10 and $n = m = 1.5$.

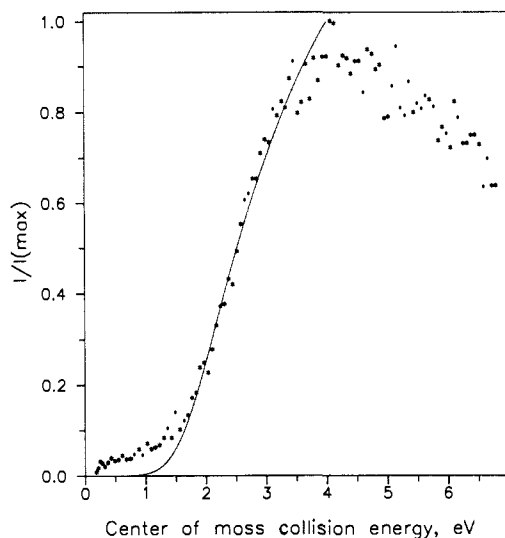
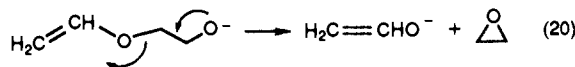


Figure 6. Appearance curve for phenyl anion from CID of benzyl alkoxide by collisions with argon gas at 5×10^{-5} Torr. The solid line is the optimized model appearance curve calculated with eq 10 and $n = m = 1.5$.

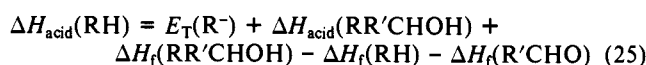
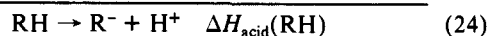
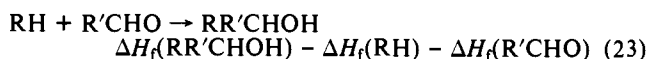
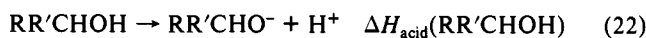
appearance curves showed tailing in the threshold region and a slow rise above threshold (for example, CID of benzyl alkoxide; Figure 6). Data that displayed this broadening were difficult to fit reliably with the cross-section models used for the carboxylates and in some cases the appearance curves were not reproducible. The reason for the different shapes of the appearance curves for products of similar dissociation processes is unclear; however, the alkoxide ions appear to be quite sensitive to the tuning conditions used at the ion sampling elements and may be internally excited by collisions in the sampling region.

The threshold energies obtained by optimization of the $n = m = 1.5$ and $n = 1, m = 0.5$ models to fit the experimental data were averaged and are given in Table III; the uncertainty quoted is 2 standard deviations. Some of the thresholds have rather large uncertainties: for example ± 0.40 eV for $\text{CH}_2=\text{CHCH}_2\text{O}^-$. This is primarily a result of the poor reproducibility of the measurements and the often poor quality of the data in terms of broadening and unreliable fits for the calculated curves. In the case of 2-(vinylloxy)ethoxide ion, the variation in the measured thresholds may be caused in part by a kinetic shift that results from a competing dissociation reaction (a competitive shift).⁵⁶ This ion dissociates by a lower energy ($E_{\text{T}} \sim 0.5$ eV) pathway to yield acetaldehyde enolate and (presumably) ethylene oxide (eq 20).⁵⁷



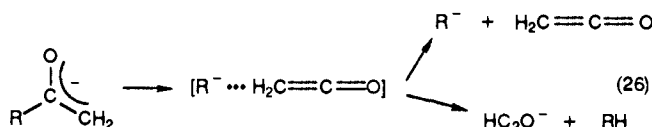
The ionic product from this lower energy fragmentation dominates the CID spectrum even above the threshold for loss of CH_2O , indicating that the cyclization is relatively fast and efficient. Thus, it may be necessary to excite the 2-(vinylloxy)ethoxide ion well above the thermochemical threshold for CH_2O loss for the rate of the latter dissociation to compete with loss of ethylene oxide.

The threshold energies measured for CID of alkoxides can be related to $\Delta H_{\text{acid}}(\text{RH})$ by means of the thermochemical cycle shown in eqs 21–25, with $\text{R}' = \text{H}$ or CH_3 . Gas-phase acidities



for RH that result from this treatment are given in Table III along with literature values where available. It can be seen that in some cases the agreement is rather poor. The two alkoxides that yield acetaldehyde as the neutral fragment from CID [i.e., $(\text{CH}_3)_2\text{CHO}^-$ and $\text{C}_6\text{H}_5\text{CH}(\text{CH}_3)\text{O}^-$] show higher threshold energies than the predicted reaction enthalpy, whereas the threshold energies for the dissociations that produce formaldehyde are often somewhat lower than predicted, with the exception of the 2-(vinylloxy)ethoxide ion and the 2-fluoroethoxide ion. It is possible that the excitation functions used for analysis of these dissociations are not appropriate, that kinetic shifts or activation barriers are causing high thresholds for secondary alkoxides, and/or that the parent ions are not actually thermal energy species due to excitation in the sampling system or inefficient cooling in the flow tube.

Threshold energies were measured for production of R^- from four ketone enolates $\text{RC}(\text{O})\text{CH}_2^-$. These ions dissociate by loss of ketene or RH (eq 26).^{24–28} The experimental appearance curves

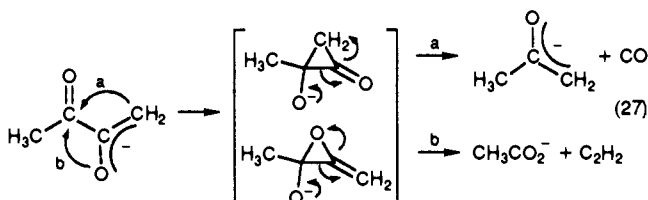


(56) Lifshitz, C.; Long, F. A. *J. Chem. Phys.* **1964**, *41*, 2468.

(57) Graul, S. T.; Squires, R. R., submitted for publication in *Int. J. Mass Spectrom. Ion Processes*.

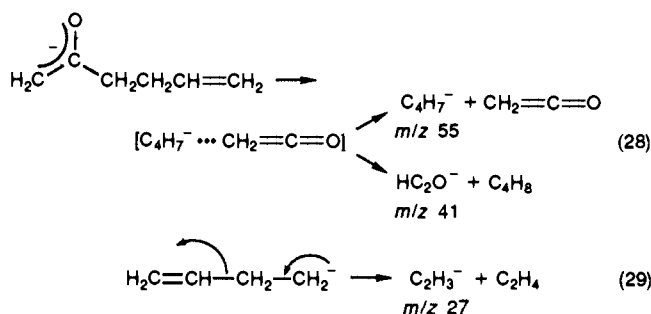
for R^- were modeled in the same manner as the data for the alkoxides and carboxylates. The threshold energies obtained from the $n = m = 1.5$ and $n = 1, m = 0.5$ models were averaged over the replicate measurements and are listed in Table IV.

In addition to CH_3CO^- and HC_2O^- , two other ionic products are observed from fragmentation of biacetyl enolate that correspond to loss of 26 and 28 amu. Both products are much less abundant than the acetyl anion or the ketenyl anion, and probably arise via a cyclization mechanism:

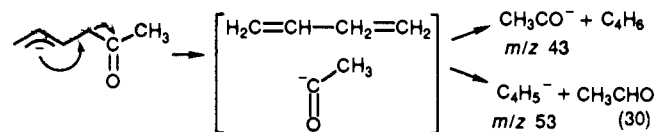


The neutral product lost in channel b is likely to be acetylene formed by a facile 1,2 hydrogen shift within the nascent vinylidene.^{58,59}

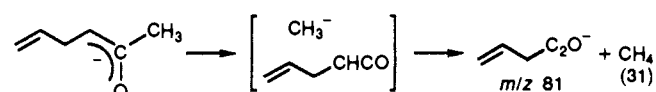
Several products are observed in the CID spectrum of deprotonated 5-hexen-2-one (allylacetone). There are three different sites in the neutral ketone that are acidic enough to be deprotonated by OH^- , and it is probable that the m/z 97 ion formed by deprotonation is a mixture of different isomers. Dissociation product ion signals are observed at m/z 81, 55, 53, 41, and 27. The major products in the collision energy range of 10–30 eV lab (3–9 eV c.m.) are the m/z 55 and 41 ions corresponding to C_4H_7^- and HC_2O^- , which probably arise from the primary enolate (eq 28). The vinyl anion (m/z 27) can arise from further decomposition of a homoallyl anion $\text{CH}_2=\text{CHCH}_2\text{CH}_2^-$ (eq 29). The



ion formed by deprotonation of allylacetone at the allylic position can dissociate upon activation by loss of butadiene to form the acetyl anion (m/z 43), or by loss of acetaldehyde to form the butadienyl anion (m/z 53) (eq 30). Finally, deprotonation can



form the secondary enolate, which can dissociate by loss of methane to form m/z 81.



The remaining ketone enolates shown in Table IV yield only R^- and HC_2O^- upon CID.

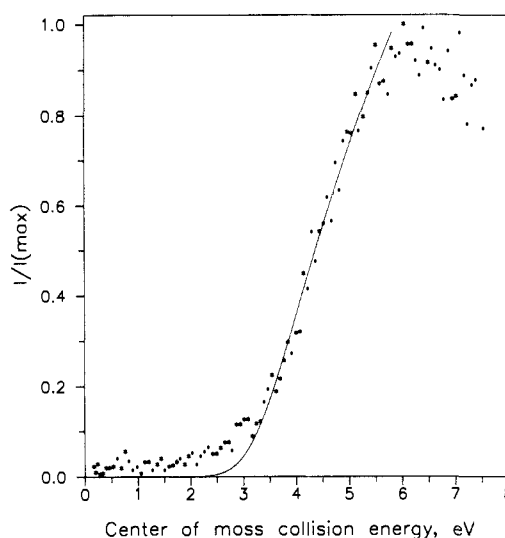
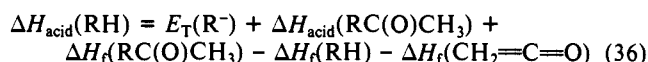
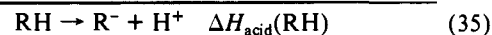
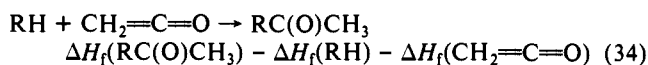
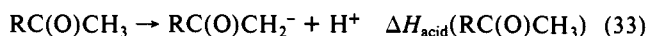
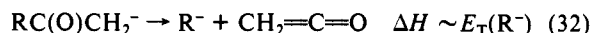


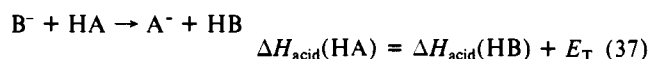
Figure 7. Appearance curve for phenyl anion from CID of acetophenone enolate by collisions with argon gas at 5×10^{-5} Torr. The solid line is the optimized model appearance curve calculated with eq 10 and $n = M = 1.5$.

The threshold energies for the production of R^- can be related to $\Delta H_{\text{acid}}(\text{RH})$ by the appropriate thermochemical cycle:



Acidities calculated from the measured threshold energies are given in Table IV, along with the pertinent thermochemical data and literature values of $\Delta H_{\text{acid}}(\text{RH})$ when available. The overall quality of the data for CID of the enolates is good [for example, CID of $\text{C}_6\text{H}_5\text{C}(\text{O})\text{CH}_2^-$ in Figure 7], and for three of the enolates studied, the agreement of the derived $\Delta H_{\text{acid}}(\text{RH})$ with literature values is within our experimental error. A notable exception is the value of $\Delta H_{\text{acid}}(\text{CH}_2=\text{CHCH}_2\text{CH}_3)$ calculated from $E_{\text{T}}(\text{C}_4\text{H}_7^-)$ for CID of allylacetone enolate. The value of 390 kcal/mol is unreasonably low for the protons of the terminal methyl group. It is interesting to note that CID of 4-pentenoate also produces C_4H_7^- with a threshold energy lower than expected (see Table II). These results, and possible reasons for the low threshold energies, are considered further in the Discussion.

Bimolecular Reactions. Threshold energies were measured for the ionic product of the endothermic proton-transfer reactions of B^- with ethylene ($\text{B}^- = \text{OH}^-, \text{CH}_3\text{O}^-, \text{CD}_3\text{O}^-, \text{and } \text{CH}_3\text{CH}_2\text{O}^-$) and with methyl fluoride ($\text{B}^- = \text{OH}^-$). For OH^- , the measured reactant ion energy distribution was narrower than the usual distributions for heavier ions; therefore, the calculated appearance curves were convoluted with a Gaussian energy distribution of 1.5 eV fwhm. For the reactions with $\text{CH}_3\text{O}^-, \text{CD}_3\text{O}^-, \text{and } \text{CH}_3\text{CH}_2\text{O}^-$, the usual energy distribution of 2 eV fwhm was used. Of the reactions studied, that of OH^- with ethylene is the most sensitive to spread in the ion energy due to the low threshold energy. The other reactions examined proved to be less sensitive to small changes (± 0.5 eV) in the width of the ion energy distribution used. The appearance curves were modeled with the same n and m parameters as used for unimolecular reactions (e.g., Figure 8); the threshold energies given by optimized fits are given in Table V. Also given are the values of $\Delta H_{\text{acid}}(\text{C}_2\text{H}_4)$ and $\Delta H_{\text{acid}}(\text{CH}_3\text{F})$ given by the relationship



(58) Krishnan, R.; Frisch, M. J.; Pople, J. A.; Schleyer, P. v. R. *Chem. Phys. Lett.* **1981**, *79*, 408.

(59) Carrington, T., Jr.; Hubbard, L. M.; Schaefer, H. F., III; Miller, W. H. *J. Chem. Phys.* **1984**, *80*, 4347.

(60) Engelking, P. C.; Ellison, G. B.; Lineberger, W. C. *J. Chem. Phys.* **1978**, *69*, 1826.

(61) Ellison, G. B.; Engelking, P. C.; Lineberger, W. C. *J. Phys. Chem.* **1982**, *86*, 4873.

well above the requisite minimum energy for loss of B^- (a competitive shift).⁵⁶

Discussion

The use of measured threshold energies to estimate reaction thermochemistry is a well-established practice that has both advantages and disadvantages.³⁸⁻⁴⁴ Among the limitations of such an approach is the fact that measurement of an appearance energy for the product of a reaction yields by definition an upper limit to the enthalpy of the process. Also, it is not always possible to define rigorously the initial state of the reactants and final states of the products of a translationally driven reaction in terms of their internal and relative kinetic energy as well as the exact structures of the species that are present in the dissociation transition state. This is particularly problematic for polyatomic species and for organic ions for which isomerization and intramolecular interactions may be important. Furthermore, threshold measurements depend upon the rates of activated reactions and therefore are susceptible to kinetic shifts.⁵⁶

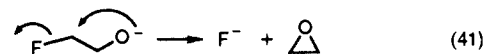
In spite of these drawbacks, useful information can be gained from determining threshold energies for endothermic reaction. A particular advantage is that such measurements provide estimates of specific bond energies that otherwise may not be determined readily. Also, because the measured threshold energy represents an activation energy, it is not sensitive to unimolecular rearrangements of the products after they separate. Estimates of thermochemical properties derived from reaction threshold energies can prove quite reliable. When the method is used to determine a thermochemical value by examining several different reactive systems, the influence of reverse activation barriers, kinetic shifts, and electronic or vibrational excitation in particular systems often can be identified. We have adopted this procedure for the present study, and further "calibrate" the method by applying it to reactions with known enthalpy changes to verify that the measured threshold energies are consistent with the thermochemistry.

The good agreement obtained between the decarboxylation threshold energies and the enthalpy of decarboxylation for the calibrant carboxylate ions (Table I) suggests that, under the present conditions, decarboxylation occurs at the thermochemical limit, i.e., there is no reverse activation energy. Several of the R^- species generated for the present study by decarboxylation have also been produced by one or more of the other methods described: by CID of alkoxides or ketone enolates or by a bimolecular reaction. Comparison of the results [i.e., $\Delta H_{\text{acid}}(\text{RH})$] obtained for the different methods provides a means to assess the reliability of the individual methods for estimating bond energies.

The methyl anion was produced by decarboxylation of acetate ion, by loss of CH_2O from ethoxide and loss of CH_3CHO from 2-propoxide, and by the nucleophilic displacement reaction of Cl^- with $\text{Me}_3\text{SiCH}=\text{CH}_2$ and $\text{Me}_3\text{SiC}_6\text{H}_5$. The threshold energies that were reported for the first three processes in an earlier paper on the reactivity of CH_3^- were derived from a linear least-squares fit to the experimental appearance curves with an additive correction for the Doppler broadening.¹⁶ These data have been reanalyzed by the method described in the Experimental Section, using eq 11 with $n = m = 1.5$ and $n = 1, m = 0$, and convoluting into the calculated appearance curve both the reactant ion energy spread and the Doppler broadening. It was necessary to collect a new appearance curve for the production of methyl anion from dissociation of 2-propoxide because the original data had an unacceptably high base line for the present analysis; this probably accounts for the increase in $E_T(\text{CH}_3^-)$ for CID of $(\text{CH}_3)_2\text{CHO}^-$ (previously reported as 2.10 ± 0.15 eV;¹⁶ herein as 2.32 ± 0.16 eV). The threshold energy for production of CH_3^- from $(\text{C}-\text{H}_3)_3\text{CO}^-$ could not be determined accurately by the present analysis due to a low signal-to-noise ratio. The linear fit used previously yielded $E_T(\text{CH}_3^-) = 1.93 \pm 0.15$ eV for CID of $(\text{C}-\text{H}_3)_3\text{CO}^-$, which corresponds to $\Delta H_{\text{acid}}(\text{CH}_4) = 414 \pm 3.5$ kcal/mol from eq 18; the uncertainty quoted reflected experimental reproducibility.¹⁶ The present analysis yields values for $\Delta H_{\text{acid}}(\text{CH}_4)$ of 419 ± 3 (acetate), 415 ± 3.5 (ethoxide), and 421 ± 3.7 kcal/mol

(2-propoxide). The average of these is 418.3 kcal/mol, in excellent agreement with the literature value of 416.8 kcal/mol.⁷ However, if the appearance energy for CH_3^- from the nucleophilic displacement reaction of Cl^- with $\text{Me}_3\text{SiCH}=\text{CH}_2$ is converted to a bond energy and hence to $\Delta H_{\text{acid}}(\text{CH}_4)$, a value of 443 kcal/mol results. Similarly, the threshold energy for the $\text{Cl}^-/\text{Me}_3\text{SiC}_6\text{H}_5$ reaction yields $\Delta H_{\text{acid}}(\text{CH}_4) = 449$ kcal/mol. The large difference between these two values and those derived from the CID reactions, and the lack of agreement with the known acidity of methane, indicate that the thresholds measured for the displacement reactions are significantly shifted to higher energies and do not reflect the thermochemistry of the reaction, as shown also in Table VI.

The fluoromethyl anion FCH_2^- was also produced by several methods: decarboxylation of $\text{FCH}_2\text{CO}_2^-$, CID of $\text{FCH}_2\text{CH}_2\text{O}^-$, and proton abstraction from CH_3F . The values of $\Delta H_{\text{acid}}(\text{CH}_3\text{F})$ derived from the decarboxylation threshold of 2.55 ± 0.22 eV [$\Delta H_{\text{acid}}(\text{CH}_3\text{F}) = 410 \pm 4.5$ kcal/mol] and the proton-transfer threshold of 0.79 ± 0.10 eV (409 ± 2.3 kcal/mol) are in excellent agreement. A recent computational study of the acidities of substituted methanes yielded $\Delta H_{\text{acid}}(\text{CH}_4) = 426.5$ kcal/mol and $\Delta H_{\text{acid}}(\text{CH}_3\text{F}) = 417.5$ kcal/mol, corresponding to a 9 kcal/mol decrease in ΔH_{acid} accompanying fluorine substitution.⁶⁵ If this decrease is applied to the experimental value for $\Delta H_{\text{acid}}(\text{CH}_4)$ of 416.6 kcal/mol,^{7,12} then the predicted $\Delta H_{\text{acid}}(\text{CH}_3\text{F})$ of 407.6 kcal/mol is in good agreement with the present results derived from decarboxylation and from proton transfer. In contrast, $\Delta H_{\text{acid}}(\text{CH}_3\text{F})$ derived from the threshold energy for formation of FCH_2^- by CID of $\text{FCH}_2\text{CH}_2\text{O}^-$ is much higher (427 kcal/mol) and corresponds to $\Delta H_f(\text{FCH}_2^-) = 2.3$ kcal/mol. However, if this heat of formation were correct, then the anion should be unbound because the radical is lower in energy with $\Delta H_f(\text{FCH}_2) = -8$ kcal/mol.⁷ Thus, the $\Delta H_{\text{acid}}(\text{CH}_3\text{F})$ derived from CID of $\text{FCH}_2\text{CH}_2\text{O}^-$ is clearly unreasonable, and the threshold energy for production of FCH_2^- must be too high. This may be a result of a kinetic shift caused by a competing lower energy fragmentation process;⁵⁶ i.e., CH_2O loss becomes competitive only when the anion is excited well above threshold. There are two dissociation processes of lower energy than loss of CH_2O and a third of comparable energy. The enthalpy for loss of H_2 is only ~ 4 kcal/mol,⁶⁶ unfortunately, we are generally unable to detect H_2 loss reliably due to broadening of the parent ion and could not determine whether this process occurred. A second low-energy dissociation pathway that is observed is dissociation to $\text{C}_2\text{H}_4\text{O}$ and F^- . The threshold energy for production of F^- is 0.93 ± 0.15 eV. The enthalpy for formation of F^- and ethylene oxide from 2-fluoroethoxide (eq 41) is 23.3 kcal/mol (1.0 eV), whereas production



of F^- and CH_3CHO is actually exothermic. Thus, the measured threshold for F^- is consistent with a cyclization process that yields F^- and ethylene oxide.⁵⁷ Loss of H^- (which we cannot detect due to the 3 amu low-mass cutoff of the triple quadrupole) is endothermic by ~ 2.1 eV, which is comparable to the enthalpy for loss of CH_2O (2.4 eV) if $\Delta H_{\text{acid}}(\text{CH}_3\text{F}) = 409$ kcal/mol.

The vinyl anion was prepared by decarboxylation of acrylate $\text{CH}_2=\text{CHCO}_2^-$, loss of CH_2O from allyl alkoxide $\text{CH}_2=\text{CHC}-\text{H}_2\text{O}^-$, loss of ketene from $\text{CH}_2=\text{CHC}(\text{O})\text{CH}_2^-$, deprotonation of ethylene, and the nucleophilic displacement reaction of Cl^- with $\text{Me}_3\text{SiCH}=\text{CH}_2$. The values of $\Delta H_{\text{acid}}(\text{C}_2\text{H}_4)$ derived from these experiments are in very good agreement for all but the displacement reaction: $\Delta H_{\text{acid}}(\text{C}_2\text{H}_4) = 408 \pm 3.5$ (acrylate), 406 ± 9.2 (allyl alkoxide), 408 ± 4.2 (methyl vinyl ketone enolate), and 405.5 kcal/mol (average of the four deprotonation reactions); compare $\Delta H_{\text{acid}}(\text{C}_2\text{H}_4) \sim 424$ kcal/mol for the $\text{Cl}^-/\text{Me}_3\text{SiCH}=\text{CH}_2$ displacement reaction. The onset for production

(65) Spitznagel, G. W.; Clark, T.; Chandrasekhar, J.; Schleyer, P. v. R. *J. Comput. Chem.* **1982**, *3*, 363.

(66) For $\Delta H_f(\text{CFH}_2\text{CHO}) = -81$ kcal/mol,⁵⁴ and $\Delta H_{\text{acid}}(\text{CFH}_2\text{CHO}) \sim 355$ kcal/mol, estimated.

of $C_2H_3^-$ from the displacement reaction is clearly shifted to too high an energy. Our results for the remaining reactions yield an average value for $\Delta H_{acid}(C_2H_4)$ of 406.8 kcal/mol, in good agreement with DePuy et al., who found $\Delta H_{acid}(C_2H_4) = 407.5$ kcal/mol.¹³

The cyclopropyl anion was produced by decarboxylation of cyclopropanecarboxylate and CID of cyclopropylmethoxide. These experiments yield $\Delta H_{acid}(\text{cyclopropane}) = 409 \pm 4.5$ and 407 ± 6 kcal/mol, respectively. This is somewhat lower than (but within experimental error of) the value determined by DePuy and co-workers of 411.5 kcal/mol.¹³ Also relevant are the results of decarboxylation of 1-methylcyclopropanecarboxylate and 2-methylcyclopropanecarboxylate ions, which suggest that α - or β -methyl substitution does not result in a substantial change in the acidity of cyclopropyl hydrogens. Our results suggest that cyclopropane is slightly more acidic than either of the methylated cyclopropanes, but the acidities for all three species are the same within experimental error. DePuy et al. found that methyl substitution on cyclopropane results in a slight enhancement of the acidity of the α -hydrogen.¹³

The C-C-C bond angle distortion in cyclopropane results in increased s-character in the C-H bonds, an effect that has been linked to enhanced acidity.⁶⁷ The increased s-character is revealed by larger ^{13}C - 1H coupling constants,^{68,69} and a correlation has been drawn between ^{13}C - 1H coupling constants and acidities in solution.⁷⁰ This correlation can be extended to gas-phase acidities of small hydrocarbons as well and, for example, correctly predicts the experimentally determined acidity of bicyclobutane ($\Delta H_{acid} = 398 \pm 2$ kcal/mol).⁷¹ The ^{13}C - 1H coupling constant for the bridging position in [1.1.1]bicyclopentane is 160 Hz,⁷² which correlates to $\Delta H_{acid} = 408$ kcal/mol. The value of ΔH_{acid} derived from the decarboxylation threshold energy for [1.1.1]bicyclopentane-1-carboxylate anion is 411 ± 3.5 kcal/mol (Table II), in good agreement with the value predicted by the coupling constant-acidity correlation.

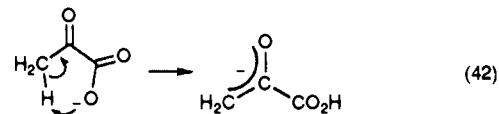
The acidity for $CH_2=CHOCH_3$ derived from the appearance energy of $CH_2=CHOCH_2^-$ from CID of $CH_2=CHOCH_2CH_2O^-$ (Table III) is higher than would be expected by comparison with the acidity of CH_3OCH_3 predicted by DePuy and co-workers: $\Delta H_{acid}(CH_3OCH_3) = 407$ kcal/mol.^{13a} The effect on acidity of replacing the methyl group in CH_3OCH_3 by a vinyl group can be estimated by comparing the predicted acidity of the primary hydrogens in propane ($\Delta H_{acid} = 415.6$ kcal/mol)¹³ with the predicted acidity of the terminal (C-4) hydrogens in 1-butene ($\Delta H_{acid} = 412.0$ kcal/mol).¹³ The enhancement of 3.6 kcal/mol observed for the substituent effect on acidity for $CH_3CH_2CH_3 \rightarrow CH_2=CHCH_2CH_3$, when applied to $CH_3OCH_3 \rightarrow CH_2=C-HOCH_3$, yields a predicted ΔH_{acid} of 403.4 kcal/mol for the methyl hydrogens in methylvinyl ether. This predicted value is significantly lower than the present value of 411 ± 12 kcal/mol, although it falls within the large experimental error for the measurement. As noted previously for the production of FCH_2^- from $FCH_2CH_2O^-$, the onset for loss of CH_2O from β -substituted ethoxide ions may be too high due to the competing, lower energy fragmentation channel that, for CID of $CH_2=CHOCH_2CH_2O^-$, yields acetaldehyde enolate and ethylene oxide.⁵⁷

The neopentyl anion was generated by decarboxylation of 3,3-dimethylbutyrate and CID of 3,3-dimethylbutoxide. These two experiments result in widely differing values of ΔH_{acid} for $C(CH_3)_4$: 417 ± 3.5 kcal/mol from decarboxylation and 405 ± 5.5 kcal/mol from CID of the alkoxide. From the C-H bond

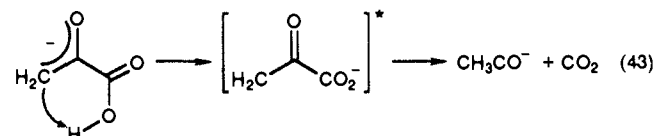
dissociation energy of neopentane (100.1 ± 2.0 kcal/mol) and the fact that we observe the anion as a bound species ($EA > 0$ eV), $\Delta H_{acid}[C(CH_3)_4]$ must be less than 414 kcal/mol (eq 1). However, it seems unlikely that $\Delta H_{acid}[C(CH_3)_4]$ would be as low as 405 kcal/mol as given by CID of the alkoxides. In the absence of additional data, we take the average of the two individual results as our "best" value: $\Delta H_{acid} = 411 \pm 10$ kcal/mol.

The phenyl anion was generated by four methods: decarboxylation of benzoate ion, CID of benzyl alkoxide and α -methylbenzyl alkoxide, loss of ketene from acetophenone enolate, and the $Cl^-/Me_3SiC_6H_5$ displacement reaction. The agreement among the derived $\Delta H_{acid}(C_6H_5)$ values is rather poor: 403 ± 3.5 (benzoate), 391 ± 5.5 (benzyl alkoxide), 403 ± 3.5 (α -methylbenzyl alkoxide), 402 ± 4.6 (acetophenone enolate), and 407 kcal/mol ($Cl^-/Me_3SiC_6H_5$ displacement). In view of the high thresholds observed for production of CH_3^- and $C_2H_3^-$ in the other displacement reactions, it seems likely that the appearance energy for $C_6H_5^-$ from $Me_3SiC_6H_5$ would also be too high and this may account for the resulting high $\Delta H_{acid}(C_6H_5)$ of 407 kcal/mol. The low value of $\Delta H_{acid}(C_6H_5)$ given by the threshold for production of $C_6H_5^-$ from benzyl alkoxide is difficult to rationalize, but may be in part a result of the poor quality of the data (see Figure 6). Other possibilities are that benzyl alkoxide is particularly susceptible to excitation in the sampling system or that some fraction of the parent ions derives from ring deprotonation. It is surprising that the results for CID of α -methylbenzyl alkoxide should differ so strongly; the threshold for production of $C_6H_5^-$ yields an acidity that agrees with the literature value, within experimental error. Similarly, the results for decarboxylation of benzoate and loss of ketene from acetophenone enolate are in good agreement with the literature value for $\Delta H_{acid}(C_6H_5)$. The results of CID of benzyl alkoxide remain a puzzle. We take as our final value for $\Delta H_{acid}(C_6H_5)$ the average of all the individual CID measurements and obtain 401 kcal/mol. (If the values from the displacement reaction and benzyl alkoxide CID are omitted, the average ΔH_{acid} is 403 kcal/mol.)

A large disparity in values of ΔH_{acid} also occurs in the data for production of the acetyl anion by decarboxylation of pyruvate and CID of 2,3-butanedione enolate: $\Delta H_{acid}(CH_3CHO) = 379 \pm 3.5$ (pyruvate) and 396 ± 3.5 kcal/mol (2,3-butanedione enolate). The accepted literature value for $\Delta H_{acid}(CH_3CHO)$ is 391 kcal/mol.⁷ The reason for the low value obtained from the decarboxylation of pyruvate is not obvious. Reactivity studies of the m/z 43 product ion with N_2O support the assignment of the acetyl anion structure; product ions are observed at m/z 59 ($CH_3CO_2^-$) and 41 (HC_2O^-), which can arise from oxygen abstraction and dehydrogenation, respectively.⁷³ The real possibility exists that some of the $C_3H_3O_3^-$ ions are not authentic pyruvate ions but the isomeric enolate ion that may arise from, for example, collision-induced isomerization of pyruvate in the sampling region (eq 42). Because the pyruvate ions are formed by fluoro-



desilylation reactions, we do not expect the enolate to be present in the flow tube. The enolate structure is undoubtedly of higher energy than the carboxylate form and, thus, could dissociate in Q2 by intramolecular proton transfer prior to loss of CO_2 to yield the acetyl anion at an anomalously low collision energy (eq 43).



If we assume that the acidity of the methyl hydrogens in pyruvic

(67) (a) Streitwieser, A., Jr.; Caldwell, R. A.; Young, W. R. *J. Am. Chem. Soc.* **1969**, *91*, 529. (b) Streitwieser, A., Jr.; Owens, P. H.; Wolf, R. A.; Williams, J. E., Jr. *J. Am. Chem. Soc.* **1974**, *96*, 5448.

(68) Foote, C. S. *Tetrahedron Lett.* **1963**, 579.

(69) (a) Wiberg, K. B. *Tetrahedron* **1968**, *24*, 1083. (b) Wiberg, K. B. In *Advances in Alicyclic Chemistry*; Hart, H., Karabatsos, G., Eds.; Academic Press: New York, 1968; Vol. 2.

(70) Battiste, M. A.; Coxon, J. M. In *The Chemistry of the Cyclopropyl Group*; Rapport, Z., Ed.; John Wiley & Sons: New York, 1987.

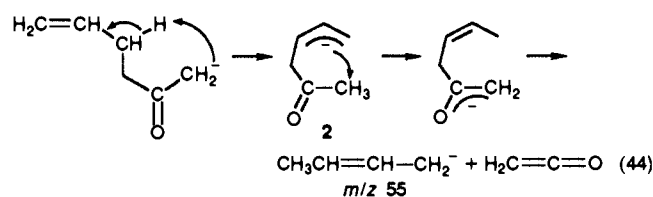
(71) Kass, S. R.; Chou, P. K. *J. Am. Chem. Soc.* **1988**, *110*, 7899.

(72) Wiberg, K. B.; Connor, D. S.; Lampman, G. M. *Tetrahedron Lett.* **1964**, 531.

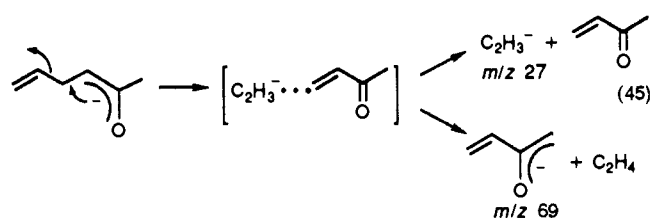
(73) Graul, S. T. Ph.D. Thesis, Purdue University, 1989.

acid is slightly greater than that of biacetyl ($\Delta H_{\text{acid}} = 356$ kcal/mol),⁵³ then we can estimate the overall enthalpy change for eq 43 to be ~ 36 kcal/mol (1.6 eV). This is close to the observed threshold energy of 1.84 eV.

There are several examples of apparently low thresholds for both decarboxylation reactions and CID of alkoxides that also may be due to the presence of higher energy isomers of the parent ions, which can dissociate to product ions of the same mass at collision energies lower than expected. For example, decarboxylation of $\text{CH}_3\text{CH}=\text{CHCO}_2^-$, $\text{CH}_2=\text{C}(\text{CH}_3)\text{CO}_2^-$, $\text{CH}_2=\text{CH}-\text{CH}_2\text{CH}_2\text{CO}_2^-$, and $(\text{CH}_3)_2\text{C}=\text{CHCO}_2^-$ occurs at collision energies lower than expected based on predicted acidities of the conjugate acids of the carbanion products. Similarly, the threshold for loss of CH_2O from $\text{CH}_3\text{CH}=\text{CHCH}_2\text{O}^-$ appears to be low. A common feature of these ions is the presence of relatively acidic hydrogens in the hydrocarbon side chains. The low thresholds could be a result either of production of the lower energy (allylic) carbanions from CID or of dissociation from a higher energy isomer of the parent ion (or perhaps both). For example, the low threshold energies observed for CID of deprotonated allylacetone may be a result of the presence of the allylic isomer **2** in the flow tube, or of an intramolecular proton transfer that converts the enolate reactant ion to **2**, which can then yield an allylic C_4H_7^- upon dissociation (eq 44). Note that the observation of vinyl anion



produced from CID of allylacetone enolate suggests that some fraction of the C_4H_7^- ions is the homoallyl isomer $\text{CH}_2=\text{CH}-\text{CH}_2\text{CH}_2^-$ (eq 29). An alternative mode of production of C_2H_3^- shown in eq 45 is possible, but seems less likely because no signal is observed at *m/z* 69.



It is particularly interesting in this context to note that the ΔH_{acid} derived for $\text{CH}_3\text{CH}_2\text{CH}=\text{CH}_2$ in Table II (408 ± 3.5 kcal/mol) is consistent with the predicted acidity of the vinylic hydrogens. Decarboxylation of $\text{CH}_3\text{CH}_2\text{CH}=\text{CHCO}_2^-$ does not display the same low threshold observed for the structurally similar carboxylates noted above. The $\text{CH}_3\text{CH}_2\text{CH}=\text{CHCO}_2^-$ ion was formed by fluorodesilylation of the trimethylsilyl ester of pure *trans*-2-pentenoic acid, and perhaps the intramolecular proton transfer is disfavored for this configuration because of the inability of the carboxyl moiety to approach the acidic allylic hydrogens of the side chain. In contrast, the crotonic acid from which $\text{CH}_3\text{CH}=\text{CHCO}_2^-$ was produced is a mixture of the *cis* and *trans* isomers. When the most acidic sites of the side chain are blocked, as in $\text{CH}_2=\text{CHC}(\text{CH}_3)_2\text{CH}_2\text{CO}_2^-$, the measured decarboxylation threshold energy yields an acidity (409 kcal/mol for the methyl protons of 3,3-dimethylbutene) that is consistent with the predictions of DePuy et al. for the acidity of the methyl group in 1-butene (412.0 kcal/mol).¹³

In the accompanying paper on the decarboxylation technique,¹⁴ we described several β -substituted ethyl anions produced by CID of the appropriate precursor carboxylate anions. Appearance energies were measured for three of these ions formed by decarboxylation: $\text{CF}_3\text{CH}_2\text{CH}_2^-$, $\text{CH}_2=\text{CHCH}_2\text{CH}_2^-$, and $\text{CH}_3\text{C}-\text{OCH}_2\text{CH}_2^-$. Due to low signal intensities, an appearance energy could not be determined for a fourth β -substituted ethyl anion, $\text{C}_6\text{H}_5\text{CH}_2\text{CH}_2^-$, from CID of the carboxylate anion. Instead, the

threshold energy was measured for production of this ion by CID of $\text{C}_6\text{H}_5\text{CH}_2\text{CH}_2\text{CH}_2\text{O}^-$ (Table III).⁷⁴ The results for $\text{CH}_2=\text{CHCH}_2\text{CH}_2^-$ are discussed above; the threshold energies appear to be low for both precursors examined, but other evidence (the observation of the vinyl anion in the CID spectrum and the reactivity studies with N_2O)⁷³ suggests that at least some of the C_4H_7^- ions are produced with the homoallyl structure $\text{CH}_2=\text{CHCH}_2\text{CH}_2^-$.

Nibbering and co-workers examined the reactivity and basicity of several C_8H_9^- ions, including the isomer formed by decarboxylation of $\text{C}_6\text{H}_5\text{CH}_2\text{CH}_2\text{CO}_2^-$.⁷⁵ They reached the conclusion that the C_8H_9^- ion is not the β -phenylethyl anion but a cyclized isomer, spiro[2.5]octadienyl anion. They estimated ΔH_{acid} for the β -hydrogens of ethylbenzene to be 406 ± 3 kcal/mol based on the branching ratio from the reaction of OH^- with $\text{C}_6\text{H}_5\text{CH}_2\text{CH}_2\text{Si}(\text{CH}_3)_3$. This prediction is in excellent agreement with the value of $\Delta H_{\text{acid}}(\text{C}_6\text{H}_5\text{CH}_2\text{CH}_3)$ of 406 ± 4.6 kcal/mol derived herein from CID of the precursor alkoxide. The C_8H_9^- ion produced by CID of $\text{C}_6\text{H}_5\text{CH}_2\text{CH}_2\text{CH}_2\text{O}^-$ may isomerize to a lower energy structure,⁷⁴ as Nibbering and co-workers demonstrated to be the case for C_8H_9^- ions formed by several other methods.⁷⁵ However, this isomerization probably occurs after the separation of the CID products, because the threshold energy for the fragmentation reflects the energy for formation of β -phenylethyl anion and CH_2O from the precursor alkoxide, rather than formation of alternative lower energy isomers.

Replacement of the methyl group in ethanol by a vinyl or a phenyl group results in a decrease in ΔH_{acid} of 4.10,⁵⁷ and 7.4 kcal/mol,⁷ respectively. By comparison, replacement of a methyl group in propane by a vinyl or a phenyl substituent results in a decrease in ΔH_{acid} of the terminal methyl hydrogens (XCH_2CH_3) of 3.6¹³ and 9.6 kcal/mol (present results). The effects of an X substituent on the acidity of the OH moiety in XCH_2OH compare reasonably well with the effect on the acidity of the CH_3 moiety in XCH_2CH_3 . Thus, we can examine the effect of a CF_3 substituent on the acidity of the alcohol to determine if the present value for $\Delta H_{\text{acid}}(\text{CF}_3\text{CH}_2\text{CH}_3)$ is reasonable. The ΔH_{acid} of $\text{CF}_3\text{CH}_2\text{OH}$ is 361.8 kcal/mol, which is 15.6 kcal/mol lower than $\Delta H_{\text{acid}}(\text{CH}_3\text{CH}_2\text{OH})$ (377.4 kcal/mol).⁷ Thus, one might predict a similar acidifying effect for replacement of CH_3 by CF_3 in propane. The value obtained for $\Delta H_{\text{acid}}(\text{CF}_3\text{CH}_2\text{CH}_3)$ from the measured decarboxylation threshold energy is 406 ± 5 kcal/mol, which is ~ 10 kcal/mol lower than the predicted $\Delta H_{\text{acid}}(\text{CH}_3\text{CH}_2\text{CH}_3)$ of 415.6 kcal/mol.¹³ This apparent CF_3 substituent effect is weaker than might be expected by comparison with the alcohols, which may be indicative of a high threshold for decarboxylation of $\text{CF}_3\text{CH}_2\text{CH}_2\text{CO}_2^-$ relative to the true enthalpy change of the reaction. As noted under Results and in the accompanying paper,¹⁴ there is a competing fragmentation pathway for the reactant ion that corresponds to HF loss and occurs with a lower activation energy. The decarboxylation threshold may therefore be shifted to higher energy.

The acidity derived for the C-4 hydrogens in butanone from the decarboxylation threshold energy for $\text{CH}_3\text{COCH}_2\text{CH}_2\text{CO}_2^-$ is 401 ± 5 kcal/mol. By comparison, the bracketed gas-phase acidity for the methyl hydrogens in 2,2-dimethylpropanal is 385 ± 6 kcal/mol.⁷⁶ With a correction of +7 kcal/mol to account for the acidifying effect of the two methyl groups,⁷⁷ and a correction of +3 kcal/mol to account for the greater inductive effect of an aldehyde group ($\sigma_1 = 0.30$) compared to an acetyl group ($\sigma_1 = 0.22$),^{4,78} one would estimate that the ΔH_{acid} of the C-4 hydrogens in butanone should be ~ 395 kcal/mol. This value is

(74) Raftery, M. J.; Bowie, J. H.; Sheldon, J. C. *J. Chem. Soc., Perkin Trans. 2* **1988**, 563.

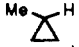


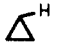

(75) Maas, W. P. M.; van Keelen, P. A.; Nibbering, N. M. M. *Org. Mass Spectrom.* **1989**, *24*, 546.

(76) (a) Noest, A. J.; Nibbering, N. M. M. *J. Am. Chem. Soc.* **1980**, *102*, 6247. (b) Peerboom, R.; Ingemann, S.; Nibbering, N. M. M. *Recl. Trav. Chim. Pays-Bas* **1985**, *104*, 74.

(77) $\Delta H_{\text{acid}}(\text{CH}_3\text{CH}_2\text{CH}_3) = 415.6$ kcal/mol and $\Delta H_{\text{acid}}[(\text{CH}_3)_3\text{CCH}_3] = 408.9$ kcal/mol.¹³ $\delta\Delta H_{\text{acid}} = -6.7$ kcal/mol.

(78) Hine, J. *Structural Effects on Equilibria in Organic Chemistry*; John Wiley & Sons: New York, 1975.

Table VII. Final Values for ΔH_{acid} Derived from the Threshold Energies of Endothermic Reactions

RH	ΔH_{acid} , kcal/mol	
	this study	lit. ^a
CH ₄	418 ± 3.5	416.8 ± 1.7
	413 ± 3.5	409.2 ± 1 ^b
	411 ± 5	
CH ₂ CHOCH ₃	411 ± 12	
C(CH ₃) ₃	411 ± 10	408.9 ± 1 ^b
	411 ± 3.5	
CH ₃ F	409 ± 4	
CH ₂ =CHC(CH ₃) ₂	409 ± 4	
	408 ± 5	411.5 ± 1 ^b
CH ₃ CH ₂ CH=CH ₂	408 ± 3.5	
C ₂ H ₄	407 ± 3	407.5 ± 1 ^b
CF ₃ CH ₂ CH ₃	398 ± 3.5	
C ₆ H ₅ CH ₂ CH ₃	406 ± 4.6	406 ± 3 ^c
CH ₃ COCH ₂ CH ₃	401 ± 4	
C ₆ H ₆	401 ± 10	400.8 ± 0.5
CH ₃ CH=CH ₂	398 ± 5 ^d	>405 ^e
CH ₃ CH=CH ₂	395 ± 5 ^d	405.8 ^b
CH ₃ CHO	387 ± 8	391 ± 2.6
(CH ₃) ₂ C=CH ₂	391 ± 3.7 ^d	
	391 ± 6 ^d	410.5 ± 1 ^b
CF ₂ H ₂	389 ± 3.5	387 ± 7
CH ₃ CH ₂ CH=CH ₂	387 ± 6 ^d	412.0 ± 1 ^b
C ₆ H ₅ CH ₃	377 ± 3.5	381 ± 2.5
CF ₃ H	376 ± 4.5	377 ± 2
CH ₃ CN	369 ± 4.5	373 ± 2.6

^aLiterature values taken from ref 7 unless otherwise noted.^bCurrent best estimates for ΔH_{acid} for these species taken from ref 13b.^cReference 75. ^dThese values are believed to be artificially low; see text. ^eReference 15.

somewhat lower than the 401 kcal/mol derived from the decarboxylation threshold, but within the combined errors.

Conclusions

The use of threshold energies for endothermic reactions to estimate thermochemical properties appears to be justified when the method is applied with caution and the results are inspected for specific effects that may cause high or low thresholds. These studies also can reveal some interesting aspects of activated dissociations or bimolecular reactions that involve polyatomic organic ions. For many of the reactions examined, the threshold energies for the product ions appear to correlate well with the reaction endothermicity. However, several exceptional cases were found. The high thresholds that were observed can be attributed to activation barriers and/or kinetic shifts caused by competing lower energy fragmentation pathways (for example, in the silane displacement reactions, and also invoked to explain the high thresholds for loss of CH₂O from CH₂=CHOCH₂CH₂O⁻ and CFH₂CH₂O⁻). Low thresholds were also observed (i.e., E_T was less than the predicted enthalpy of reaction) and were often associated with species in which there was some potential for

isomerization in the parent ion due to the presence of acidic hydrogens in the side chain. A higher energy isomer of the parent ion may yield the same carbanion species expected from CID of the lower energy isomer if the isomerization is readily reversible. The occurrence of an exothermic rearrangement of the higher energy form to the lower energy form during dissociation would yield an anomalously low appearance energy for the carbanion. Alternatively, the product ion that is actually formed upon CID may be a lower energy isomer of the predicted product ion accessed by a dissociation mechanism with a low activation energy. Further reactivity studies should help to clarify this situation.

For the most part, the decarboxylation method appears to be reliable for prediction of gas-phase acidities, and for the small sample of ions studied, CID of ketone enolates also gave good results. The acidities derived from thresholds for CID of alkoxides were less satisfactory and the overall reproducibility was somewhat poorer than that of the other methods. An additional problem that can be encountered with both alkoxide and ketone enolate ions is nonselective deprotonation of the neutral alcohol or ketone; it may be advantageous to produce these species by a more specific method such as fluorodesilylation reactions.

From the complete results, we obtain the final values for gas-phase acidities listed in Table VII; included for comparison are accepted literature values for ΔH_{acid} where available, or the current best estimates. Species examined for which the threshold energy of unimolecular dissociation yielded unreasonably low values for ΔH_{acid} included CH₃C(O)CO₂⁻, CH₂=C(CH₃)CO₂⁻, (CH₂)₂CHCH₂CO₂⁻, (CH₃)₂C=CHCO₂⁻, CH₂=CHCH₂CH₂CO₂⁻, C₆H₅CH₂O⁻, and the carboxylate and alkoxide precursors for CH₃CH=CH⁻. Dissociation of an isomeric form of the parent ion seems a probable cause for many of the low threshold energies observed.

Acknowledgment. This research was supported by grants from the National Science Foundation (CHE-8502515 and CHE-8815502) and by the Donors of the Petroleum Research Fund, administered by the American Chemical Society. We wish to thank Mr. Dingneng Wang for implementing in our laboratory the CRUNCH program kindly supplied by Professor Peter Armentrout for threshold energy data analysis. R.R.S. thanks the Alfred P. Sloan Foundation for a fellowship and S.T.G. is grateful to Rohm and Haas for a graduate fellowship administered by the Organic Division of the American Chemical Society.

Registry No. CF₃CO₂⁻, 14477-72-6; CH₃CO₂⁻, 71-50-1; NCCH₂CO₂⁻, 23297-32-7; C₆H₅CO₂⁻, 766-76-7; CF₃H, 75-46-7; CF₂H₂, 75-10-5; CFH₃, 593-53-3; CH₄, 74-82-8; CH₃CN, 75-05-8; C₂H₄, 74-85-1; CH₃CHO, 75-07-0; CF₃CH₂CH₃, 421-07-8; CH₃CH=CH₂, 115-07-1; (CH₃)₂C=CH₂, 115-11-7; CH₂=CHCH₂CH₃, 106-98-9; CH₃COCH₂CH₃, 78-93-3; C(CH₃)₄, 463-82-1; C₆H₆, 71-43-2; CH₂=CHC(CH₃)₃, 558-37-2; C₆H₅CH₃, 108-88-3; CH₂=CHOCH₃, 107-25-5; C₆H₅CH₂C-H₃, 100-41-4; CH₃CH₂O⁻, 16331-64-9; (CH₃)₂CHO⁻, 15520-32-8; FCH₂CH₂O⁻, 74279-90-6; CH₂=CHCH₂O⁻, 71695-00-6; (CH₃)₂CHC-H₂O⁻, 35730-34-8; CH₃CH=CH₂CH₂O⁻, 125251-09-4; CH₂=CHOC-H₂CH₂O⁻, 125251-10-7; (CH₃)₃CCH₂CH₂O⁻, 125251-11-8; C₆H₅CH₂O⁻, 45581-66-6; C₆H₅CH(CH₃)O⁻, 113534-04-6; C₆H₅CH₂CH₂CH₂O⁻, 116982-19-5; CH₂=CHC(O⁻)=CH₂, 125251-12-9; CH₃COC(O⁻)=C-H₂, 125251-13-0; CH₂=CHCH₂CH₂C(O⁻)=CH₂, 125251-14-1; C₆-H₅C(O⁻)=CH₂, 34172-40-2; Me₃SiCH=CH₂, 754-05-2; Me₃SiC₆H₅, 768-32-1; cyclopropane, 75-19-4; methylcyclopropane, 594-11-6; bicyclo[1.1.1]pentane, 311-75-1.